Intracellular pH modulates vimentin remodeling in response to oxidants

Alma E. Martínez, Patricia González-Jiménez, Cristina Vidal-Verdú, María A. Pajares,

Dolores Pérez-Sala*

Department of Structural and Chemical Biology, Centro de Investigaciones Biológicas Margarita Salas, C.S.I.C., 28040 Madrid, Spain

*To whom correspondence should be addressed at: Centro de Investigaciones Biológicas Margarita Salas, C.S.I.C., Ramiro de Maeztu, 9, 28040 Madrid, Spain. Email: dperezsala@cib.csic.es

Running title: Effect of pH on vimentin response to oxidants

Abstract

The intermediate filament protein vimentin plays key roles in the integration of cytoskeletal functions with impact on essential cellular processes including migration, mitosis and autophagy. Moreover, vimentin is involved in pathological processes such as cancer, fibrosis and interaction with pathogens. The vimentin network is finely tuned by posttranslational modifications, among which, those affecting its single cysteine residue (C328) play a critical role not only in vimentin function, but also in its interplay with actin. Interestingly, C328 exhibits a low pKa, which favors the presence of the thiol group in the thiolate form, and therefore its reactivity, at physiological pH. Therefore, C328 reactivity and modifications could be modulated by pH fluctuations in the physiological range. Here we show that indeed, vimentin cysteine oxidation and alkylation, and the subsequent vimentin remodeling, can be modulated as a function of pH, in vitro and in cells. Lowering intracellular pH by several means renders vimentin unresponsive to disruption by oxidants, whereas provoking an intracellular alkalinization exerts a sensitizing effect. The protective effect of low pH appears selective for vimentin since it does not preclude oxidant-elicited disruption of actin or tubulin structures. Importantly, a C328A vimentin mutant is resistant to disruption by oxidants under all pH conditions, highlighting the role of the thiol group at this position in the pH-dependent modulation of vimentin susceptibility to oxidants. Taken together, these results put forward intracellular pH as a key factor modulating redox-dependent vimentin remodeling.

Keywords

Thiol group ionization, cysteine mutants, intermediate filaments, intracellular pH, structural disruption, oxidative protein modifications

Abbreviations: EIPA, 5-(N-ethyl-N-isopropyl)amiloride; Mal-B, Maleimide-PEG$_2$-Biotin; pHi, intracellular pH; TRITC, tetramethylrhodamine B isothiocyanate

Introduction

The intermediate filament protein vimentin plays key roles in cell architecture and mechanotransduction [1-3]. Nevertheless, at least equally important are its roles in the integration of cellular structures and signaling pathways, with consequences on organelle homeostasis, regulation of autophagy, and lipid metabolism, as well as its key role in the cellular response to various kinds of stress [4-7]. Indeed, although vimentin may seem dispensable for some processes under control conditions, its whole features and functions are revealed under stress situations. Thus, vimentin-deficient mice show compromised wound healing, smaller size, vascular dysfunction and altered responses to infection, among other phenotypes [7].

The assembly of vimentin into filaments is a complex process not completely elucidated. The current models propose the formation of parallel vimentin dimers, which then form staggered antiparallel tetramers. A variable number of tetramers, eight or ten, depending on the models, would associate laterally to form unit length filaments which would connect end to end to form the filaments [8-11]. Vimentin filaments are highly dynamic structures, which can elongate through the addition of subunits at either end, exchange subunits at any point along their length, severe into fragments and fuse again in cells [12, 13]. This dynamic behavior is required for efficient reorganization in response to stress, including oxidative stress [14].

Interestingly, oxidants and electrophiles elicit profound alterations of vimentin filaments in vitro and of the vimentin network in cells, which depend on the structural features of the agents employed [14, 15]. Importantly, the single cysteine residue of this protein, C328, is a key target for various posttranslational modifications, and appears necessary for vimentin reorganization under oxidative or electrophilic stress [4]. Moreover, cysteine-dependent vimentin remodeling during stress impacts the organization of other cytoskeletal elements, namely actin stress fibers, thus participating in cytoskeletal interplay [15].

Vimentin C328 has been identified as a hot spot for posttranslational modifications in proteomic studies [16], and at least fourteen different modifications have been detected to date, with non-overlapping functional consequences [17-19] (see [20] for review). Certain modifications by small moieties, including nitrosation, appear to have mild consequences on filament assembly, whereas bulkier moieties can elicit more intense disruption and even filament severing [19]. On the other hand, readily reversible modifications, such as glutathionylation, independently of their immediate consequences, have been proposed to act as protective mechanisms avoiding excessive oxidative damage, whereas more stable modifications, such as lipoxidation or oxidation to sulfonic acid, may require new protein synthesis for restoration of filament or network morphology. Interestingly, the study of several C328 mutants revealed that introduction of different side chains at this position elicits distinct morphological network rearrangements, thus supporting the functional importance of local perturbations at this site [15].

Cysteine modification plays a key role in redox signaling and transmission of oxidative stress responses [21, 22]. Reactive cysteine residues involved in regulatory processes usually display a low pKa. We have recently determined that C328 in purified human vimentin presents two ionization curves yielding pKas of approximately 4.5 and 7.4, respectively, which suggests the existence of two cysteine populations [23]. This also implies that near physiological pH (7.2-7.4) a significant proportion of C328 residues (>50%) would be in the most reactive, thiolate form [24]. Therefore, if a similar ionization behavior takes place in cells, changes in intracellular pH in the physiological range could induce significant differences in the reactivity of the C328

population with pKa 7.4, and therefore in their extent of modification and subsequent vimentin reorganization.

Importantly, an intracellular pH (pHi) of approximately 7.2 is considered normal for cells in culture, whereas tumor cells display a more alkaline pH (between 7.3 and 7.6) [25]. In addition, broad pHi variations can occur under certain physiological and pathophysiological conditions, as well as in response to drugs, affecting the whole cell or specific subcellular compartments. For instance, apoptosis by growth factor deprivation in certain cell lines is accompanied by a marked intracellular acidification (pHi<6.8, [26]). Similarly, during high intensity exercise the pH of muscle cells can reach values below 6.8 [27], and intense acidifications have also been reported in several models of hypoxia or ischemia [28, 29]. Conversely, examples of intracellular alkalinization include the effect of mitogens, which increase pHi by 0.1 to 0.3 pH units [30], anaphylatoxin (complement C5a), which causes pHi increases of 0.3-0.4 pH units in neutrophils in models of sepsis [31], antipsychotic drugs that increase the pHi of astrocytes [32], and the rise in pHi occurring during malignant transformation by certain oncogenes [33]. Indeed, alkaline pHi confers cancer cells an advantage for proliferation and invasiveness [34, 35]. Therefore, inducing intracellular acidification has been envisaged as a promising strategy to elicit cancer cell toxicity per se or to sensitize tumor cells to the action of certain drugs used in chemotherapy [34, 36-38]. Lastly, temporal pHi variations occur within single cells depending on the cell cycle [39, 40], whereas spatial pHi variations include those between distinct organelles, with the mitochondrial matrix being the most basic [41-43], as well as the intracellular gradients formed for instance during migration [42, 44].

Here, we have monitored the effect of pH on vimentin C328 modifications and disruption by oxidants, both in vitro and in cells. Our results confirm that vimentin responsiveness to oxidative and electrophilic insults is strongly dependent on the pH of the environment, through mechanisms requiring C328, which indicates the importance of the presence of a thiol group at this position. Therefore, these observations unveil a previously underestimated factor contributing to the regulation of this intermediate filament.

Materials and methods

Reagents. HEPES, Pipes, urea, 2-mercaptoethanol, 5-(N-ethyl-N-isopropyl)amiloride (EIPA), syrosingopine and diamide were from Merck; Tris was obtained from VWR; DTT, pHrhodo™ Red, and EZ-Link™ Maleimide-PEG2-Biotin (Mal-B) were from Thermo Fisher Scientific; H_2O_2 was from ChemCruz; Precision Plus Protein Dual Color Standards and Sypro Ruby were from BioRad. Anti-vimentin V9 (sc-6260) in its unconjugated, Alexa488 and agarose conjugated versions was from Santa Cruz Biotechnology. Rabbit anti-α-tubulin antibody (ab52866) was from Abcam. Alexa 647 anti-rabbit (A-21244) was from Thermo Fisher Scientific. Mouse TrueBlot ULTRA secondary antibody was from Rockland Immunochemicals. Immobilon-P membranes were from Millipore.

Protein preparation. Recombinant human vimentin wild type (wt), purified essentially as described [45] was obtained from Biomedal (Spain) or from Abvance (Spain). The protein in 8 M urea, 5 mM Tris-HCl pH 7.6, 1 mM EDTA, 10 mM 2-mercaptoethanol, 0.4 mM PMSF and approximately 0.2 M KCl was ultrafiltrated using Millipore Amicon Ultra filter units (10 K pore size) and dialyzed step-wise in 5 mM Pipes-Na pH 7.0, 1 mM DTT containing decreasing urea concentrations (8, 6, and 2 M). Final dialysis was performed for 16 h at 16 °C in 5 mM Pipes-Na pH 7.0 and 0.25 mM DTT [46]. The ultrafiltration step was necessary for efficient removal of EDTA [46]. The buffer from the last dialysis was kept and the protein concentration was

estimated from its A_{280}, using an extinction coefficient of 22450M^{-1} cm^{-1}. Refolded protein was subsequently subjected to DTT removal or stored directly in aliquots at -80 °C until use. For DTT elimination, vimentin underwent three cycles of 1:20 dilution with 5 mM Pipes-Na pH 7.0 and ultrafiltration on Amicon Ultra filter units in order to reach a theoretical DTT concentration of 30 nM.

***In vitro* modification of vimentin by oxidants and electrophiles at different pHs.** The pH-dependent modification of refolded vimentin was assessed by gel-based techniques. Briefly, vimentin at 4 µM diluted with buffers at different pHs, and incubated at 24 °C in the presence of 1 mM H_2O_2 or 1 mM diamide for 1 h, or with 20 µM Mal-B for 15 min. The buffers at different pHs used were near the pK_a values previously calculated by us [23]. Given the fact that DTT can react with electrophilic compounds and chelate metals [47], reactions with Mal-B were carried out with vimentin subjected to DTT elimination, while for modifications with diamide and H_2O_2, the final concentration of DTT was kept below 0.1 mM. In addition, it is to note that the incubation time with Mal-B was reduced to prevent its degradation, since the hydrolysis rate of this compound increases with pH and temperature [48].

Reactions were stopped by boiling in Laemmli sample buffer containing 5% (v/v) 2-mercaptoethanol (reducing conditions) or in the absence of reductant (non-reducing conditions) and proteins were analyzed by SDS-PAGE on 10% (w/v) polyacrylamide gels. Then, proteins incubated with Mal-B were electrotransferred to PVDF membranes using a Trans-blot SD semi-dry transfer cell (Bio-Rad). Biotin incorporation was assessed by incubating blots with HRP-streptavidin (1:1000 v/v, GE Healthcare) and vimentin levels were estimated by western blot as described below. On the other hand, vimentin oligomerization after treatment with H_2O_2 or diamide was analyzed by SDS-PAGE followed by protein staining. Briefly, gels were fixed with 40% (v/v) methanol and 10% (v/v) acetic acid for at least 1 h, stained with Sypro Ruby from 90 min to 3 h, washed with 10% (v/v) methanol and 6% (v/v) acetic acid, and visualized under UV light on a Gel-Doc XR Imaging System (Bio-Rad). All the aforementioned steps were performed under gentle agitation and, importantly, the gel was protected from light as of the staining step. Signal intensities were evaluated by image scanning and analysis with ScionImage.

Optical microscopy of purified vimentin structures. Vimentin at 4 µM was incubated in 10 mM HEPES pH 7.0 or 8.0, 0.1 mM DTT, in the absence or presence of 1 mM diamide for 1 h at room temperature. At the end of the treatment, vimentin polymerization was elicited by addition of 150 mM NaCl, final concentration, and the incubation was continued for 1 h at room temperature. Subsequently, anti-vimentin V9 antibody (1:200 v/v) was added for 30 min, followed by anti-mouse-Alexa 488 (1:200 v/v) for an additional 30 min. Aliquots from the incubation mixtures were deposited on coverslips, allowed to dry and mounted on glass slides with Fluorsave. Vimentin structures were visualized by fluorescence microscopy on a Leica SP5 microscope.

Cell culture and treatments. SW13/cl.2 vimentin-deficient cells were the generous gift of Dr. A. Sarriá (University of Zaragoza, Spain) [49]. HeLa cells were originally from ATCC and were authenticated by microsatellite amplification (short tandem repeat (STR)-PCR profiling) at Secugen, S.L. (Madrid, Spain). Primary human dermal fibroblasts (ref. GM00409) were obtained from the NIGMS Human Genetic Cell Repository at the Coriell Institute for Medical Research (Camden, NJ). They were cultured in DMEM with 10% (v/v) fetal bovine serum (FBS, from Sigma or Gibco) and antibiotics (100 U/ml penicillin and 100 µg/ml streptomycin). MEF *Vim(-/-)* were the generous gift of Prof. John Eriksson (Abo Academy University, Turku, Finland). Treatments were generally performed in serum-free medium. Unless stated otherwise, cells were treated

with 1 mM diamide for 15 min, either directly of after preincubation with 25 µM EIPA for 15 min, 10 µM monensin for 5 min, 10 µM syrosingopine for 1 h. Treatment with H_2O_2 was carried out at 1 mM for 25 min. For treatment in acidic or in alkaline medium, 12 mM HCl or 6.25 mM NaOH, final concentrations, respectively, were added to DMEM containing 10 µM nigericin, and the cell culture medium was replaced with this mixture immediately before the addition of diamide. For some experiments, cells were seeded on 6-well plates containing one coverslip at the bottom of each well, as previously described [50]. After treatments, cells on coverslips were fixed and used for microscopy and cells attached to the wells were used for protein analysis, as described below.

Plasmids and transfections. The RFP//vimentin wt and C328A mutant plasmids for expression of the red fluorescent protein DsRed-Express2 and vimentin as separate products, have been previously described [4, 15]. mCherry-SEpHluorin was a gift from Prof. Sergio Grinstein (Addgene plasmid # 32001; http://n2t.net/addgene:32001; RRID:Addgene_32001) [51]. SW13/cl.2 cells were transfected with mCherry-SEpHluorin using Lipofectamine 2000 (Invitrogen), following the instructions of the manufacturer. SW13/cl.2 cells stably transfected with expression vectors for vimentin wt or C328A (RFP//vimentin wt or C328A), have been previously described [15].

Cell lysis and western blot. Cells were washed with cold PBS and lysed in 50 mM Tris–HCl pH 7.5, 0.1 mM EDTA, 0.1 mM EGTA, 0.1 mM β-mercaptoethanol, containing 0.5% (w/v) SDS, 0.1 mM sodium orthovanadate and protease inhibitors (2 µg/ml each of leupeptin, aprotinin and trypsin inhibitor, and 1.3 mM Pefablock), by gentle scraping and forced passes through a 26 1/2G needle on ice. Protein concentration in lysates was determined by the bicinchoninic acid (BCA) method (ThermoFisher Scientific). Lysates were denatured at 95 ◦C for 5 min in Laemmli buffer and aliquots containing 30 µg of protein were separated on 10% (w/v) SDS-polyacrylamide gels. Proteins were transferred to Immobilon-P membranes (Millipore) using a semi-dry transfer system (Bio-Rad) and a three-buffer system following the instructions of the manufacturer. Blots were blocked with 2% (w/v) powdered skimmed milk in T-TBS (20 mM Tris-HCl, pH 7.5, 500 mM NaCl, 0.05% (v/v) Tween-20). Antibodies were diluted in 1% (w/v) BSA in T-TBS. Primary antibodies were routinely used at 1:1000 dilution, followed by HRP-conjugated secondary antibodies (Dako) at 1:2000 dilution. Bands of interest were visualized by enhanced chemiluminescence detection using the ECL system (Cytiva), exposing blots to X-Ray film (Agfa).

Vimentin immunoprecipitation. SW13/cl.2 cells stably transfected with RFP//vimentin wt were incubated in control conditions or with diamide (1 mM final concentration for 15 min), and lysed as described above using a non-reducing lysis buffer (without β-mercaptoethanol) containing 10 mM Mal-B for free thiol labelling. Lysates from control and diamide treated cells were then incubated for 30 min at room temperature. Aliquots of lysates containing 150 µg of protein were diluted with lysis buffer containing 1% (w/v) NP-40 instead of SDS to diminish the SDS concentration to 0.1% (w/v). Samples were then incubated overnight with anti-vimentin V9-agarose for immunoprecipitation at 4ºC. Beads were washed four times with cold PBS by centrifugation at 14,000 g for 1 min at 4ºC, and subsequently boiled in Laemmli buffer during 5 min to elute the retained proteins. Eluted proteins were collected by centrifugation at 14,000 g for 2 min at room temperature. The immunoprecipitated products were separated by SDS-PAGE and transferred to PVDF. Mal-B incorporation was detected by incubation with HRP-streptavidin (1:5000 v/v), and the position of vimentin was confirmed by western blot using Mouse TrueBlot ULTRA as secondary antibody.

Immunofluorescence and confocal microscopy. Cells on coverslips or on glass bottom dishes were washed twice with PBS and incubated in 4% (w/v) paraformaldehyde (PFA) in PBS for 25

min at room temperature. Fixed cells were permeabilized with 0.1% (v/v) Triton X-100 in PBS for 20 min at room temperature, and blocked with 1% (w/v) BSA in PBS for 1 h. This blocking solution was also used for antibody dilutions. For vimentin detection, cells were incubated with Alexa488-conjugated anti-vimentin antibody (1:200 v/v) for 1 h, whereas for tubulin detection, anti- α-tubulin antibody (1:400 v/v) was used for 1 h followed by Alexa-647 conjugated secondary antibody (1:400 v/v) dilution for an additional hour. F-actin was detected by incubation of fixed and permeabilized cells with 0.25 µg/ml phalloidin tetramethylrhodamine B isothiocyanate (phalloidin-TRITC, Sigma) in blocking solution. Where indicated, nuclei were counterstained with 2.5 µg/ml 4´,6-diamidino-2-phenylindol (DAPI) for 1 h. Images were acquired on SP5 or SP8 Leica confocal microscopes, using 63× magnification, routinely every 0.5 µm.

Image analysis. For image analysis, Leica LasX software or Image J (FIJI) were used. Figures show single sections of images or overlay projections are shown, as indicated in the corresponding figure legends. For estimation of vimentin filament disruption, the "Analyze Particles" command of Image J was used to monitor the number of particles in the experimental conditions.

Estimation of intracellular pH. Variations in pHi under the assay conditions were confirmed by monitoring the fluorescence of SW13/cl.2 cells transfected with mCherry-SEpHluorin, a ratiometric pHi indicator protein, in which mCherry fluorescence is stable at several pH, whereas SEpHluorin fluorescence is very acid-labile, resulting in a decrease in green/red fluorescence ratio at acidic pH [51]. For pHi calculations, red and green fluorescence was acquired using excitation wavelengths of 561 and 488 nm, respectively, and emission between 572 and 635 nm for red and 505 and 550 nm for green fluorescence. To convert the green/red ratio from the experimental conditions into pHi values, a standard curve was generated by measuring the SEpHluorin and mCherry fluorescence intensities of mCherry-SEpHluorin-transfected cells incubated in a K^+-rich buffer (25 mM HEPES, 145 mM KCl, 0.8 mM $MgCl_2$, 1.8 mM $CaCl_2$, 5.5 mM glucose) containing nigericine and adjusted to three different pH values (6.9, 7. 5, and 8.5), thus causing pHi to match the extracellular pH. Measurements were carried out either on a Leica SP8 microscope equipped with a CO_2 and thermostatized chamber or on a Widefield Multidimensional Microscopy System Leica AF6000 LX for live cell imaging. In addition, pHrodo Red (Invitrogen) was used as an indicator of pHi, following the instructions of the manufacturer. Briefly, cells were washed once with live cell imaging solution (LCIS: 20 mM HEPES, pH 7.4, 140 mM NaCl, 25 mM KCl, 1.8 mM $CaCl_2$, 1 mM $MgCl_2$) and incubated with the pHrodo Red staining solution (pHrodo Red 1:2000 v/v in LCIS) at 37°C for 30 min. Then, cells were washed with DMEM and were cultured under the indicated experimental conditions. For pHi calculations, live cells were imaged on a Widefield Multidimensional Microscopy System Leica AF6000 LX using the Texas Red filter.

Statistical analysis. Unless otherwise stated, all experiments were repeated at least three times and results are shown as average values ± standard error of mean (SEM). GraphPad Prism 8.0 software was used to perform the statistical analysis. For comparisons of multiple data sets the one-way analysis of variance (ANOVA) followed by Tukey's multiple comparison test was used. For comparison between two groups of data, the Student's t-test for unpaired samples was used. Statistically significant differences are indicated on the graphs and/or in the figure legends, as follows: *$p<0.05$, **$p<0.01$, ***$p<0.001$, ****$p<0.0001$. The number of determinations for each experimental condition or the sample size are given in the corresponding figure legends.

Results

Oxidative modifications and alkylation of vimentin C328 in vitro are dependent on pH. Vimentin C328 can be modified in vitro by oxidants and electrophiles. In our previous work, we detected the existence of two C328 populations in purified vimentin, one of which exhibits a pKa of approximately 7.4 [23], suggesting that C328 modifications could depend on pH variations in the physiological range. As we reported earlier [23], incubation of vimentin in the presence of the general oxidant H_2O_2 or of the cysteine-selective oxidant diamide leads to an increase in the levels of a vimentin oligomer detectable by SDS-PAGE only under non-reducing conditions (Fig. 1A and B), which is compatible with a disulfide-linked vimentin dimer, as previously characterized [52]. The apparent size of this dimer is higher than expected, reportedly due to the high proportion of α-helix in the protein structure and the potential occurrence of extended conformations [52]. Here we incubated vimentin with oxidants at pH between 7.0 and 8.0 and monitored the levels of the disulfide-linked vimentin dimer as an index of C328 oxidation. Interestingly, the formation of the H_2O_2-elicited oxidized dimer increased with the pH of the incubation mixture in the 7.0-8.0 pH range (Fig. 1A). Similarly, vimentin oligomerization elicited by treatment with the oxidant diamide was moderately improved at pH 8.0 (Fig. 1B). In addition, we monitored vimentin C328 alkylation by incubation of the protein with Mal-B. The intensity of the biotin signal associated with vimentin was 2.5-fold higher at pH 8.0 than at pH 7.0, thus confirming that C328 alkylation also increased within this pH range (Fig. 1C).

We have previously shown that vimentin oxidation disrupts filament assembly in vitro [14]. Here, we assessed the effect of pH on optically detectable vimentin structures employing an immunolabeling strategy, as described in [53]. Samples of vimentin polymerized under control conditions (pH 7.0) showed numerous regular lineal structures over a clean background on which some small protein aggregates could also be observed (Fig. 1D). Preincubation with diamide before polymerization resulted in the appearance of a higher background of disorganized protein, together with globular aggregates surrounded by some filamentous structures. Preincubation at pH 8.0 in the absence of diamide already resulted in the appearance of some background protein aggregates in addition to filaments. Notably, both the presence of background protein and the size of the amorphous and globular aggregates increased after preincubation with diamide at pH 8.0 (Fig. 1D). Incubation mixtures treated in the same way, but excluding vimentin only showed a dark background (Fig. 1D, upper right), whereas bright field observation of diamide-treated vimentin samples not immunostained with antibodies clearly showed the presence of aggregates (Fig. 1D, lower right). Taken together, these results show that changes in pH modulate vimentin susceptibility to modification and disruption by oxidants in vitro.

Diamide-elicited disruption of the cellular vimentin network depends on pHi. We have previously reported that diamide profoundly disrupts the cellular vimentin network causing a fragmentation of vimentin filaments into dots in several cell types [4, 14, 15]. This effect is readily detectable by fluorescence microscopy after a few minutes of treatment and affects 80% to 90% of the cell population [14]. Here, we observed that treatment of SW13/cl.2 cells stably expressing vimentin wt with diamide for increasing times progressively altered cellular vimentin, resulting in the appearance of bright dots after a 15 min treatment, which later evolved towards a diffuse cytoplasmic background, indicative of vimentin disassembly and/or solubilization (Fig. 2A). This effect was very obvious after 2 h treatment, as illustrated in the fluorescence intensity profile (Fig. 2A, graph).

To explore whether this effect could be modulated by pHi, we treated cells with diamide for 15 min at the regular pH of the cell culture medium (~7.5), or in acidic or alkaline medium supplemented with the proton ionophore nigericin to promote the equilibration between extracellular and intracellular pH. Treatment in acidic medium (pH 6.9) suppressed diamide-induced vimentin disruption, as evidenced by the preservation of intact filaments (Fig. 2B). Conversely, alkaline conditions (pH 8.5) potentiated the effect of diamide, leading to disassembly of vimentin to an extent similar to that achieved after 2 h of treatment at the regular pH. Diamide is stable and modifies cysteine residues over a wide range of pH, for which changes in its effect should not be ascribed to alterations in its chemical stability or reactivity [54]. Remarkably, variations of pH per se, that is, in the absence of diamide (Fig. 2B, left images), did not impair filament integrity to any appreciable extent, even under high pHi conditions (pH 8.5). Variations in pHi under the assay conditions were confirmed by monitoring the fluorescence of the ratiometric pHi indicator construct mCherry-SEpHluorin [51], transfected into SW13/cl.2 cells (Fig. 2C).

To rule out that the striking rearrangement of vimentin filaments into dots and diffuse structures could be related to protein degradation, we examined the integrity of the protein by western blot of cell lysates obtained under the same experimental conditions. As shown in Figure 2D, western blot of these lysates with antibodies directed towards the N- or the C-terminal domains of the protein, namely, antibodies D21H3 and V9, with epitopes located around residues R45 and N417, respectively, confirmed the preservation of the size of the full length protein and the absence of degradation products under all conditions. Therefore, the drastic disruption of the vimentin network observed upon treatment with diamide at neutral and alkaline pHi was not caused by vimentin protein degradation, and could be attributed to filament fragmentation and/or solubilization.

We have recently reported that H_2O_2 disrupts vimentin organization in cells by mechanisms dependent, at least in part, on the presence of C328 [15]. Interestingly, vimentin network disruption by H_2O_2 was also sensitive to pHi (Suppl. Fig. 1). H_2O_2 treatment elicited heterogeneous alterations of the vimentin network with the frequent appearance of bundles and/or juxtanuclear accumulations (Suppl. Fig. 1). Whereas these alterations appeared attenuated at acidic pH, treatment at alkaline pH clearly potentiated vimentin disruption by H_2O_2, leading not only to vimentin accumulations, but also to the appearance of cells with filament fragments and/or diffuse vimentin (Suppl. Fig. 1). Therefore, these observations indicate that the susceptibility of the vimentin network to disruption by various oxidants in cells strongly depends on pHi.

Acidic pHi does not protect actin or microtubules against diamide-elicited disruption. To explore whether variations in pHi affect the susceptibility of other cytoskeletal structures to disruption by oxidants, we first assessed the effect of diamide on f-actin distribution and its potential modulation by changes in pHi. In control cells, f-actin was typically distributed both at the cell cortex, where it displayed small protrusions compatible with focal adhesions, and in the cytoplasm, where it appeared mainly as short fibers of irregular orientation distributed throughout the cell (Fig. 3A). Some subcortical stress fibers could also be detected. In overall projections, the intensity of f-actin staining was rather homogeneous across the cell (Fig. 3A). Interestingly, treatment of cells with diamide elicited a characteristic alteration of the f-actin pattern, with the appearance of a thin defined actin cortex with some focal adhesions, and a cytoplasmic mesh of diffuse structures with a “sponge-like” pattern (Fig. 3A). Remarkably, the intensity of f-actin staining was greatly decreased in the region corresponding to the nucleus,

which was clearly recognizable in overall projections. This effect could be easily appreciated in fluorescence intensity profiles (Fig. 3A, graph). The effect of diamide on f-actin distribution under different pHi conditions is shown in Fig. 3B. Interestingly, acidic or alkaline pH conditions per se did not elicit a significant perturbation of the distribution of actin into small fibrils. Notably, acidic conditions, shown above to protect vimentin filaments from diamide-elicited fragmentation, did not prevent actin disruption by diamide. Therefore, cells treated with diamide at acidic pHi still showed a decrease in f-actin staining in the region corresponding to the nucleus, and a sponge-like pattern of actin structures in the cytoplasm (Fig. 3B). Treatment of cells with diamide at alkaline pHi rendered similar observations, with an intense disruption of actin distribution (Fig. 3B).

Diamide treatment also profoundly altered microtubules, which lost their homogenous distribution and appeared as diffuse structures together with some remaining misoriented microtubules (Fig. 3C, diamide, inset). In this case, as observed for actin, neither acidic nor alkaline pH protected microtubules from the effect of diamide (Fig. 3C). Acidic or alkaline pH did not elicit significant alterations of microtubules per se. The organization of vimentin is shown here for comparison, to illustrate the typical protection of vimentin filamentous structures at acidic pH, coexisting with deeply disrupted microtubules.

Thus, the modulatory effect of pH on oxidant-elicited disruption of cytoskeletal structures appears to be selective for vimentin.

Vimentin disruption by diamide is modulated by inhibitors of transporters affecting pHi. Intracellular pH is subjected to a tight control involving numerous transporters [30, 42]. Pharmacological modulation of these transporters can drastically alter pHi. Therefore, as a complementary strategy to evidence the importance of pHi in vimentin disruption by oxidants we elicited variations in pHi employing pharmacological strategies. EIPA is an inhibitor of the Na^+/H^+ antiporter which causes intracellular acidification [55, 56]. Preincubation of cells with this inhibitor clearly protected the vimentin network from diamide-elicited disruption (Fig. 4A). Also, syrosingopine, which causes intracellular acidification by inhibiting the lactate transporter [57], achieved a partial protection of filament integrity under the conditions employed. Conversely, the H^+ ionophore monensin, which causes intracellular alkalinization [58], markedly potentiated the effect of diamide, leading to vimentin disassembly (Fig. 4A) analogous to that observed by treatment in alkaline pH (shown in Fig. 2B). To estimate the severity of vimentin disruption, we quantitated the number of vimentin filament fragments or particles per cell under the various experimental conditions (Fig. 4B). Diamide significantly increased the number of filament fragments with respect to control. Both EIPA and syrosingopine prevented the effect of diamide, whereas monensin clearly amplified filament disruption by diamide, as reflected by a 2-fold increase in the number of particles with respect to diamide alone (Fig. 4B). Of note, none of the compounds employed disrupted vimentin filament integrity per se, although monensin induced a partial accumulation of filaments near the center of the cell (Fig. 4A). Monitoring mCherry-SEpHluoring fluorescence upon treatment with the various agents, confirmed the occurrence of an intracellular acidification in the presence of EIPA and syrosingopine, and an intracellular alkalinization after treatment with monensin, as estimated from the ratio of green to red fluorescence (Fig. 4C).

In addition to modulation of the activity of proton transporters, the simple alteration the pH of the cell culture medium has been used as a strategy to elicit variations in pHi [59, 60]. In particular, mild extracellular acidosis has been shown to induce intracellular acidification [61]. Consistent with this, culturing cells in RPMI1640, pH 7.5 or in HBSS, pH 7.6 allowed fast vimentin

filament fragmentation into dots upon diamide treatment (Suppl. Fig. 2A). In contrast, incubation in PBS-glucose, pH 7.3, blunted this effect (Suppl. Fig. 2A). As previously observed for other strategies inducing intracellular acidification, the protective effect of incubation in PBS was selective for vimentin, since f-actin distribution suffered the typical diamide provoked alterations in all incubation media (Suppl. Fig. 2B).

Vimentin C328 modification in cells is modulated by pHi. The protective effect of acidic pHi on vimentin disruption by oxidants could be due to a lower proportion of the C328 thiol group in its thiolate, reactive form, under these conditions, which could correlate with a lower susceptibility of this group to chemical modification, as shown above for in vitro assays. Therefore, we assessed the impact of modulators of pHi on the extent of C328 modification in response to diamide. Diamide has been reported to induce diverse oxidative modifications in cells, including protein inter- or intra-molecular disulfide crosslinks [62], various forms of S-thiolation, such as glutathionylation, cysteinylation or CoAlation [63-66], as well as potentially more severe oxidations under conditions of sustained oxidative stress [63]. All these modifications imply a loss of free thiol groups in the protein. Therefore, we have estimated the proportion of vimentin with a free thiol group as an inverse index of the extent of C328 modification, as schematized in Fig. 5A. For this, cells were treated in the absence or presence of diamide, and immediately collected and lysed in buffer containing Mal-B to label free thiol groups. Subsequent vimentin immunoprecipitation and biotin detection revealed that, as expected, diamide treatment significantly decreased Mal-B incorporation into vimentin and consequently, free-thiol content (Fig. 5B). Moreover, we could confirm that pretreatment with EIPA preserved, whereas monensin further decreased vimentin free thiol content with respect to the effect of diamide alone (Fig. 5C). Taken together, these results are consistent with lower extent of C328 modification at acidic pHi, and the opposite at alkaline pHi, and therefore suggest that pHi modulation has an impact on diamide-induced oxidation of the vimentin thiol group.

Variations in pHi modulate the disruption of endogenous vimentin by oxidants in several cell types. The alteration of the vimentin network by cysteine-reactive agents has been evidenced in numerous cell lines and primary cells [4, 67, 68]. Here, we explored its potential modulation by pHi in several cell types (Fig. 6). In HeLa epithelial cancer cells, diamide elicited an extensive fragmentation of vimentin filaments into dots, which tended to accumulate at the center of the cell (Fig. 6A). Consistent with the observations in SW13/cl.2 cells, the effect of diamide was attenuated by lowering pHi by means of incubation at low extracellular pH in the presence of nigericin or by pretreatment with EIPA. In sharp contrast, diamide elicited vimentin disruption was potentiated by rising pHi by treatment in alkaline medium supplemented with nigericin or by pretreatment with monensin. Thus, the combination of diamide and monensin led to diffuse disassembled vimentin coexisting with vimentin dots and some filament remnants. Variations of pHi in this cell type elicited by various strategies were estimated and confirmed using pHrodo (Suppl. Fig. 3).

Diamide also elicited a clear fragmentation of vimentin into dots, in primary human fibroblasts, an effect that was more obvious at the peripheral areas of the cell (Fig. 6B). In this cell type, incubation in acidic pH medium plus nigericin or treatment with EIPA elicited a marked protective effect, as vimentin dots were not detected and filament continuity was preserved. Conversely, incubation with diamide at alkaline pH or in combination with monensin resulted in the appearance of a diffuse vimentin background, indicative of disassembly in extensive areas of the cell (Fig. 6B). Additionally, the modulation of the effect of diamide by pHi variations was confirmed in MEF *Vim(-/-)* transfected with human vimentin (Suppl. Fig. 4A), which showed a

clear protection of vimentin fragmentation by EIPA and a potentiation of vimentin disruption by monensin.

Altogether the modulatory effect of pHi on vimentin disruption by diamide was confirmed in several cell types, all of which showed a protective effect of acidic pHi and a worsening effect of alkaline pHi.

C328 is required for diamide-elicited vimentin disruption at several pHi. We have previously showed that vimentin single cysteine residue, C328, is required for disruption by diamide. To explore the importance of C328 thiol group for the modulation of network disruption by pHi, we monitored the effect of diamide at different pHi in cells expressing the vimentin C328A mutant. As previously reported by us, vimentin C328A filaments were resistant to diamide-elicited disruption (Fig. 7A). Importantly, integrity of the vimentin C328A filament network was preserved not only under control and acidic conditions, but also upon incubation at alkaline pHi (Fig. 7A), a condition in which vimentin wt filaments are profoundly fragmented and disassembled (Fig. 2A and 4A). As an additional control of the importance of vimentin C328 under these conditions, we confirmed that vimentin C328A filaments were also completely protected from fragmentation by diamide in the presence of monensin (Fig. 7A). Therefore, these observations suggest that C328, with its reactive thiol group, plays a key role in the remodeling of vimentin by oxidants, as well as in the differential response of vimentin to oxidants at various pHi.

Interestingly, although vimentin C328A was protected from the effect of diamide, actin was still susceptible to diamide disruption in cells expressing this cysteine-deficient vimentin mutant (Fig. 7B). Therefore, in diamide-treated cells, f-actin displayed the typical decrease in f-actin staining in the region corresponding to the nucleus, together with a reticular or diffuse cytoplasmic pattern (Fig. 7B). These observations confirm that substituting vimentin C328 by a non-nucleophilic amino acid, selectively protects vimentin, but not other cytoskeletal structures, against the effect of diamide, and its modulation by pH changes.

Finally, the importance of C328 was confirmed in MEF *Vim(-/-)* transfected with vimentin wt or C328A. In this cell type, only vimentin wt was susceptible to filament fragmentation by diamide, which was attenuated by EIPA and potentiated by monensin, whereas vimentin C328A formed filaments under all experimental conditions (Suppl. Fig. 4).

Discussion

The intermediate filament protein vimentin is emerging as a key target of oxidative and electrophilic compounds [20]. Its single cysteine residue, C328, has been found to be modified by numerous moieties, including endogenous oxidants and electrophiles, as well as natural compounds and drug metabolites [4, 14, 15, 19, 69]. The relatively low pKa of this cysteine makes it susceptible to modification under pathophysiological conditions, as well as potentially sensitive to changes in pH. Here we show that variations in pH modulate C328 modification by oxidants and electrophiles, both in vitro and in cells. Acidic pH conditions, which would reduce the proportion of the C328 thiol in its reactive thiolate form, protect the protein from modification and the vimentin filament network from disruption by oxidants, whereas alkaline pH conditions, which would favor thiolate formation, elicit the opposite effect. Therefore, these observations unveil a novel factor in the regulation of the response of vimentin to redox

alterations. A scheme of the hypothesized changes in cysteine ionization and modification depending on pH is depicted in Fig. 8.

Cysteine residues are key elements in redox signaling [21]. Although cysteine residues are not abundant in proteins, many of them are highly conserved and entail important functions. Their high nucleophilicity is at the basis of their ability to form covalent adducts with numerous electrophiles and therefore, of being preferred sites for a variety of posttranslational modifications. Cysteine reactivity towards specific agents is determined by several factors, including accessibility, the potential for hydrophobic interactions or formation of complexes, and pKa [70, 71]. Cysteine pKa depends in turn on the environment, particularly on the presence of protonated carboxylic residues and/or hydrogen bonds donors in the vicinity of the cysteine [72, 73]. Cysteines with low pKa are typically present in proteins involved in and/or susceptible to redox regulation, including thioredoxin, glutaredoxin, protein tyrosine phosphatases, etc. (reviewed in [72]). In this context two considerations should be made, first, a low pKa implies a higher proportion of the thiolate at physiological pH, but sometimes lower nucleophilicity, and second, protein features can increase thiol reactivity towards selective agents but not in an indiscriminate manner [70]. There are several examples of the modulation of cysteine susceptibility to oxidation or alkylation by pH variations in vitro, including the oxidation of protein tyrosine phosphatases [74], and the inactivation of glutaredoxin by iodoacetamide [75]. However, although the reactivity of cysteine residues in cells is widely assumed to depend on pHi, examples of this modulation in the cellular context are scarce.

Type III intermediate filaments possess a cysteine residue that is conserved in all members of this class and across species [76]. In addition, the sequence in the vicinity of this residue is highly conserved, with several acidic residues as well as potential targets for phosphorylation [76]. Previous results from our group on the pKa of C328 in purified human vimentin are compatible with the existence of two distinct thiol populations, one that is largely ionized at physiological pH and another with a pKa falling within physiological pH range (~ 7.4) [23]. The results herein presented show that the modification of purified vimentin by oxidants and cysteine-reactive compounds is indeed modulated by changes in pH from 7.0 to 8.0, with alkaline pH favoring a more extensive modification. Moreover, monitoring vimentin polymerization by optical microscopy shows that, under our conditions, alkaline pH worsens the formation of filamentous structures per se and potentiates the aggregation of the protein induced by diamide.

Intracellular pH is subjected to ample variations, both in a spatial and stimulus-dependent manner [42]. With respect to organelle pH, lysosomes are the most acidic compartments, with intraluminal pH of ~ 4.5 in mature lysosomes. Mitochondria are the most alkaline organelles with a matrix pH of 7.8, whereas the nucleus and endoplasmic reticulum display a neutral pH (7.2) [42]. Moreover, in migrating cells, a pHi gradient has been characterized with a higher pH value at the leading edge (front) [44]. In addition, significant pHi variations have been measured during the cell cycle, upon stimulation with growth factors, or in cells undergoing apoptosis [40, 56, 77]. Therefore, the possibility exists that vimentin oxidation or lipoxidation are modulated by pHi.

As a proof of concept for this hypothesis, first we have used the model cell line SW13/cl.2 stably transfected with human vimentin, in which pHi has been modulated by means of ionophores. These initial approaches have clearly shown that acidic pH protects vimentin filaments from disruption by oxidants known to target C328 (diamide and H_2O_2 [4, 14, 15, 23]), whereas alkaline pH potentiates their deleterious effect. Notably, vimentin disruption by diamide occurs in several cell culture media that maintain a pH close to 7.4, including DMEM, RPMI1640 and HBSS,

but it does not take place in PBS, pH 7.3. Nevertheless, it should be noted that alterations in pHi can have broad cellular consequences, including inhibition of mitochondrial respiration, [27], for which the contribution of additional mechanisms to the modulation of vimentin disruption under various pHi conditions cannot be excluded. Conversely, metabolic alterations such as inhibition of the mitochondrial respiratory chain or induction of apoptosis by growth factor deprivation of toxic compounds, can elicit pHi alterations [26]. For these reasons, here we have used a variety of strategies to modulate pHi, acting through diverse mechanisms, in order to ensure that the effects observed were most likely attributable to changes in pHi.

Importantly, the pHi-dependence of vimentin disruption could also be observed upon pharmacological modulation of pHi. In particular, the inhibitor of the Na^+/H^+ antiporter EIPA, which induces intracellular acidification [55, 56], protected vimentin filaments from diamide-elicited disruption. A protective effect on filament integrity was also observed with syrosingopine, an inhibitor of the MCT1/4 transporters (lactate/proton symporter monocarboxylate transporter), which also elicits intracellular acidification by provoking lactate retention [57]. Thus, whereas diamide treatment resulted in total fragmentation of filaments into dots, the combination of diamide and syrosingopine only induced an incipient disassembly. In sharp contrast, the ionophore monensin, which causes an intracellular alkalinization [58], markedly potentiated diamide-elicited disruption leading to the appearance of multiple small dots and a diffuse vimentin pattern, similar to the effect of basic extracellular pH combined with nigericin.

These pharmacological strategies allowed the estimation of the free thiols remaining in vimentin after treatment with diamide under the various pHi conditions. This indicated that the extent of vimentin oxidation by diamide was decreased at acidic pHi and potentiated under alkaline conditions, respectively, as revealed by the corresponding inverse changes in the availability of free thiols. However, strategies to assess the proportion of “free cysteine thiols” in a protein could entail several interpretations, given the complexity and interchangeability of cysteine modifications. Theoretically, oxidation of a certain proportion of C328 residues in the filament could paradoxically increase overall C328 reactivity, for instance by opening the filament conformation and making more cysteine residues accessible for modification, or by promoting the formation of sulfenic acids, which are more reactive, or of disulfide bonds that can be interchanged. Indeed, cysteine modification can lead to protein unfolding [78], and we have observed that certain modifications of C328 increase the width of single vimentin filaments in vitro [14]. Reciprocally, in certain proteins, stretching or mechanical unfolding can increase cysteine accessibility and modification [79], which in turn can regulate the properties of the protein [80]. Indeed, vimentin C328 shows increased labeling with a cysteine-reactive fluorophore upon cell “relaxation” with blebbistatin [81], whereas C522 in nuclear lamin A is exposed under mechanical stress [82]. Also, network reorganization in response to other stimuli could expose or shield cysteine residues. From the functional point of view, certain vimentin modifications could be compatible with filament assembly and, if reversible, even protect the protein from more deleterious modifications. In fact, we have previously observed that even under control conditions there is a certain degree of reversible vimentin C328 oxidation [15, 16], which could correspond to glutathionylation, persulfidation or other modifications [16, 83]. In fact, in a previous work, we observed an increase in the proportion of unmodified C328 after short-term nitroxidative stress, suggesting a shuttling of the modifications or conformational changes with exposure of unmodified C328 [16].

Most oxidants, including diamide and H_2O_2 also alter actin structures and microtubules [4, 84, 85]. Interestingly, the protective effect of acidic pH observed in this work appears to be selective for vimentin since neither actin nor tubulin networks were protected from diamide-elicited disruption by lowering pHi. Indeed, actin disruption occurred in all cell culture media tested. This situates vimentin filaments as cellular structures specially predisposed to the modulation of their oxidative modifications by pHi changes.

Importantly, the actin cytoskeleton is considered one of the main pH-sensitive systems in cells [86]. The modulation of actin structures by cellular pH is known to occur through various mechanisms. Several actin regulatory proteins are regulated by pHi. For instance, cofilin, which elicits actin depolymerization, is more active at alkaline pH [87, 88]. Also, actin depolymerizing factor (ADF) shows higher actin binding activity at basic pH. At focal adhesions, talin binding to f-actin decreases at pH above 7.2, allowing fast focal adhesion turnover and cell migration (for a review see [86] and references therein). Nevertheless, to the best of our knowledge, it is not clear whether pH regulation of actin dynamics involves a differential susceptibility to oxidation of any of these components.

Moreover, it should be taken into account that pHi could affect the susceptibility to oxidation of other cellular proteins. Of particular interest for our topic, various protein kinases and phosphatases are regulated by redox mechanisms, and their activation/inactivation could be modulated by pHi. For instance, both PKA and PKG are regulated by oxidation [89], as well as Aurora kinase [90]. In addition, certain protein phosphatases possess cysteine residues with low pKa, which are susceptible of modification by oxidants and electrophiles, which inhibit their enzymatic activity. This would result in hyperphosphorylation of certain proteins, and potentially vimentin, thus contributing to its disassembly [91]. Therefore, the changes elicited by certain oxidants on the vimentin network could be due to the combined action of oxidation and phosphorylation. Indeed, we have previously observed that treatment of cells with calyculin A, an inhibitor of protein phosphatases 1 and 2A, increases the levels of vimentin phosphorylated at S72 and the proportion of soluble vimentin, and potentiates diamide elicited disruption [14]. In this way, vimentin could behave as a coincidence-regulated sensor or coincidence detector, as proposed for other proteins including β-catenin and cofilin [35]. Indeed, cofilin is activated by deprotonation of a critical histidine residue (H133) and dephosphorylation of S3 at alkaline pHi. In turn, β-catenin undergoes deprotonation of H36 and phosphorylation of S33 and S37 and this, favors binding of ubiquitin ligase and degradation. In this context, the observation that a vimentin C328A mutant is not disrupted by oxidants at any pHi indicates that the cysteine residue plays an important role in this potential sensing mechanism. On the other hand, our previous observation that elimination of 11 phosphorylation sites in the vimentin N-terminal (head) domain (vimentin SA mutant) partially protects filaments from disruption by diamide [14] could favor this hypothesis, which will require additional studies. In fact, a potential bidirectional interplay between oxidation and phosphorylation could exist since phosphorylation can influence the reactivity or accessibility of cysteine residues [92, 93], and in turn, cysteine modification could influence phosphorylation at other sites.

The results herein reported are consistent with a modulatory effect of pHi on vimentin disruption, and point to the involvement of C328 in this effect. A very strong argument supporting our interpretation relies on the use of the vimentin C328A mutant, which is not sensitive to diamide-elicited disruption, even at alkaline pHi, highlighting the need of a thiol group in this position for vimentin remodeling, even under these extreme conditions. The involvement of C328 in these effects could be related to its modification by various moieties,

the occurrence of modifications in its environment and/or to its presence in an ionized or non-ionized form that could contribute to alter the charge of the filament. This in turn, could affect assembly and interactions.

Oxidant-elicited disruption of vimentin was modulated by strategies altering pHi in several cell types, including both primary cells, such as human dermal fibroblasts and MEF *Vim(-/-)* transfected with human vimentin, as well as tumor cell lines, such as HeLa. This suggests that pH modulation of vimentin oxidative modifications may be a general mechanism, although it needs to be considered that certain oxidants can elicit pHi alterations in a cell-type and subcellular compartment dependent manner [94-96]. These alterations could influence C328 reactivity and therefore vimentin remodeling. In addition, elements of the antioxidant response, including antioxidant enzymes and glutathione levels also depend on the cell type and cellular compartment (reviewed in [97, 98]), and some of them could be modulated by pHi, thus contributing to the final outcome.

Variations in pHi could affect vimentin mechanics. Indeed, in vitro studies have shown that pH influences the mechanical properties of single vimentin filaments, which may be related to an effect on electrostatic interactions between subunits within filaments [99], and/or with cations (e.g. Zn^{2+}, Mg^{2+}) [23]. This could also affect the accessibility of C328 and its susceptibility to modification. Importantly, although cysteine pKa is an important factor determining reactivity, other factors should be considered that could influence susceptibility to oxidation. In certain cases, pH variations can elicit conformational changes that influence cysteine accessibility or reactivity [100].

The regulation of vimentin disassembly by the combined action of oxidants and pHi variations could have important cellular implications, both in health and disease. The higher pHi of tumoral cells [25] could contribute to higher vimentin dynamics in response to redox changes. A relatively alkaline pH is known to exist at the cell front during migration [44]. In combination with the local generation of ROS [101], this could contribute to create conditions favorable for vimentin disassembly that occurs at the leading edge, which is known to be required for the formation of lamellipodia [102]. Moreover, these observations highlight the importance of vimentin C328 as a key regulator of its response to oxidants and electrophiles. Other type III intermediate filaments, which also have an equivalent single cysteine, may function in a similar manner. Nevertheless, mutants at the single cysteine residues or bearing additional cysteines, as well as peripherin, which possesses two cysteines residues may behave differently.

In summary, our results reinforce the role of the single, conserved cysteine residue of vimentin in filament and network organization, and propose that it may concomitantly respond to redox status and pHi variations, thus contributing to the complex mechanisms of vimentin regulation in cells.

Funding. This work was supported by Grants RTI2018-097624-B-I00 and PID2021-126827OB-I00, funded by MCIN /AEI/10.13039/501100011033 and ERDF, A way of making Europe; RETIC Aradyal RD16/0006/0021 from ISCIII, cofunded by ERDF; AEM is the recipient of a Juan de la Cierva postdoctoral contract FJC2021-047028-I funded by MCIN/AEI/ 10.13039/501100011033 and European Union NextGenerationEU/PRTR; PGJ is the recipient of a predoctoral contract PRE2019-088194, from MCIN/AEI /10.13039/501100011033 and ESF, Investing in your future", CVV has been the recipient of a fellowship JAEIntroICU-2021- LifeHub-03, from the network PIE-202120E047-Conexiones-Life (CSIC), Spain.

Acknowledgements

Feedback from EpiLipidNet (CA19105) is gratefully acknowledged. We thank the personnel of the Optical Microscopy facility at Centro de Investigaciones Biológicas Margarita Salas for their advice.

References

[1] A.E. Patteson, A. Vahabikashi, R.D. Goldman, P.A. Janmey, Mechanical and Non-Mechanical Functions of Filamentous and Non-Filamentous Vimentin, Bioessays 42(11) (2020) e2000078.
[2] A.B. Ndiaye, G.H. Koenderink, M. Shemesh, Intermediate Filaments in Cellular Mechanoresponsiveness: Mediating Cytoskeletal Crosstalk From Membrane to Nucleus and Back, Frontiers in cell and developmental biology 10 (2022) 882037.
[3] P. Shah, C.W. McGuigan, S. Cheng, C. Vanpouille-Box, S. Demaria, R.S. Weiss, J. Lammerding, ATM Modulates Nuclear Mechanics by Regulating Lamin A Levels, Frontiers in cell and developmental biology 10 (2022) 875132.
[4] D. Pérez-Sala, C.L. Oeste, A.E. Martínez, B. Garzón, M.J. Carrasco, F.J. Cañada, Vimentin filament organization and stress sensing depend on its single cysteine residue and zinc binding, Nat Commun 6 (2015) 7287.
[5] P. Mohanasundaram, L.S. Coelho-Rato, M.K. Modi, M. Urbanska, F. Lautenschlager, F. Cheng, J.E. Eriksson, Cytoskeletal vimentin regulates cell size and autophagy through mTORC1 signaling, PLoS Biol 20(9) (2022) e3001737.
[6] W.J. Shen, S.K. Zaidi, S. Patel, Y. Cortez, M. Ueno, R. Azhar, S. Azhar, F.B. Kraemer, Ablation of vimentin results in defective steroidogenesis, Endocrinology 153(7) (2012) 3249-57.
[7] K.M. Ridge, J.E. Eriksson, M. Pekny, R.D. Goldman, Roles of vimentin in health and disease, Genes Dev 36(7-8) (2022) 391-407.
[8] N. Mucke, T. Wedig, A. Burer, L.N. Marekov, P.M. Steinert, J. Langowski, U. Aebi, H. Herrmann, Molecular and biophysical characterization of assembly-starter units of human vimentin, J Mol Biol 340(1) (2004) 97-114.
[9] H. Herrmann, U. Aebi, Intermediate Filaments: Structure and Assembly, Cold Spring Harbor perspectives in biology 8(11) (2016) a018242.
[10] S.A. Eldirany, I.B. Lomakin, M. Ho, C.G. Bunick, Recent insight into intermediate filament structure, Curr Opin Cell Biol 68 (2021) 132-143.
[11] M. Eibauer, M.S. Weber, R. Kronenberg-Tenga, C.T. Beales, R. Boujemaa-Paterski, Y. Turgay, S. Sivagurunathan, J. Kraxner, S. Köster, R.D. Goldman, O. Medalia, Vimentin filaments integrate low complexity domains in a highly complex helical structure, BioRxiv (2023) doi: 10.1101/2023.05.22.541714.
[12] G. Colakoglu, A. Brown, Intermediate filaments exchange subunits along their length and elongate by end-to-end annealing, J Cell Biol 185(5) (2009) 769-77.
[13] F. Nunes Vicente, M. Lelek, J.Y. Tinevez, Q.D. Tran, G. Pehau-Arnaudet, C. Zimmer, S. Etienne-Manneville, G. Giannone, C. Leduc, Molecular organization and mechanics of single vimentin filaments revealed by super-resolution imaging, Sci Adv 8(8) (2022) eabm2696.
[14] A. Mónico, S. Duarte, M.A. Pajares, D. Pérez-Sala, Vimentin disruption by lipoxidation and electrophiles: role of the cysteine residue and filament dynamics, Redox Biol 23 (2019) 101098.
[15] P. González-Jiménez, S. Duarte, A. Martínez-Fernández, E. Navarro-Carrasco, V. Lalioti, M.A. Pajares, D. Pérez-Sala, Vimentin single cysteine residue acts as a tunable sensor for network organization and as a key for actin remodeling in response to oxidants and electrophiles, Redox Biol 64 (2023) 102756.

[16] E. Griesser, V. Vemula, A. Mónico, D. Pérez-Sala, M. Fedorova, Dynamic posttranslational modifications of cytoskeletal proteins unveil hot spots under nitroxidative stress, Redox Biol 44 (2021) 102014.
[17] K. Stamatakis, F.J. Sánchez-Gómez, D. Pérez-Sala, Identification of novel protein targets for modification by 15-deoxy-D12,14-prostaglandin J2 in mesangial cells reveals multiple interactions with the cytoskeleton., J Am Soc Nephrol 17 (2006) 89-98.
[18] D. Frescas, C.M. Roux, S. Aygun-Sunar, A.S. Gleiberman, P. Krasnov, O.V. Kurnasov, E. Strom, L.P. Virtuoso, M. Wrobel, A.L. Osterman, M.P. Antoch, V. Mett, O.B. Chernova, A.V. Gudkov, Senescent cells expose and secrete an oxidized form of membrane-bound vimentin as revealed by a natural polyreactive antibody, Proc Natl Acad Sci U S A 114(9) (2017) E1668-E1677.
[19] M. Kaus-Drobek, N. Mucke, R.H. Szczepanowski, T. Wedig, M. Czarnocki-Cieciura, M. Polakowska, H. Herrmann, A. Wyslouch-Cieszynska, M. Dadlez, Vimentin S-glutathionylation at Cys328 inhibits filament elongation and induces severing of mature filaments in vitro, FEBS J 287 (2020) 5304-5322.
[20] A. Viedma-Poyatos, M.A. Pajares, D. Pérez-Sala, Type III intermediate filaments as targets and effectors of electrophiles and oxidants, Redox Biol 36 (2020) 101582.
[21] J.M. Held, Redox Systems Biology: Harnessing the Sentinels of the Cysteine Redoxome, Antioxid Redox Signal 32(10) (2020) 659-676.
[22] H. Sies, D.P. Jones, Reactive oxygen species (ROS) as pleiotropic physiological signalling agents, Nat Rev Mol Cell Biol 21(7) (2020) 363-383.
[23] A. Mónico, J. Guzman-Caldentey, M.A. Pajares, S. Martin-Santamaria, D. Pérez-Sala, Molecular Insight into the Regulation of Vimentin by Cysteine Modifications and Zinc Binding, Antioxidants (Basel) 10(7) (2021) 1039.
[24] S.B. Wall, J.Y. Oh, A.R. Diers, A. Landar, Oxidative modification of proteins: an emerging mechanism of cell signaling, Frontiers in physiology 3 (2012) 369.
[25] K.A. White, B.K. Grillo-Hill, D.L. Barber, Cancer cell behaviors mediated by dysregulated pH dynamics at a glance, J Cell Sci 130(4) (2017) 663-669.
[26] A. Rebollo, J. Gómez, A.M.d. Aragón, P. Lastres, A. Silva, D. Pérez-Sala, Apoptosis Induced by IL-2 Withdrawal is Associated with an Intracellular Acidification, Experimental Cell Research 218 (1995) 581-585.
[27] A.J. Genders, S.D. Martin, S.L. McGee, D.J. Bishop, A physiological drop in pH decreases mitochondrial respiration, and HDAC and Akt signaling, in L6 myocytes, Am J Physiol Cell Physiol 316(3) (2019) C404-C414.
[28] G.J. Gores, A.L. Nieminen, B.E. Wray, B. Herman, J.J. Lemasters, Intracellular pH during "chemical hypoxia" in cultured rat hepatocytes. Protection by intracellular acidosis against the onset of cell death, J Clin Invest 83(2) (1989) 386-96.
[29] H. Hagberg, Intracellular pH during ischemia in skeletal muscle: relationship to membrane potential, extracellular pH, tissue lactic acid and ATP, Pflugers Arch 404(4) (1985) 342-7.
[30] W.H. Moolenaar, Effects of growth factors on intracellular pH regulation, Annu Rev Physiol 48 (1986) 363-76.
[31] S. Denk, M.D. Neher, D.A.C. Messerer, R. Wiegner, B. Nilsson, D. Rittirsch, K. Nilsson-Ekdahl, S. Weckbach, A. Ignatius, M. Kalbitz, F. Gebhard, M.E. Weiss, J. Vogt, P. Radermacher, J. Kohl, J.D. Lambris, M.S. Huber-Lang, Complement C5a Functions as a Master Switch for the pH Balance in Neutrophils Exerting Fundamental Immunometabolic Effects, J Immunol 198(12) (2017) 4846-4854.
[32] J. Ren, D. Song, Q. Bai, A. Verkhratsky, L. Peng, Fluoxetine induces alkalinization of astroglial cytosol through stimulation of sodium-hydrogen exchanger 1: dissection of intracellular signaling pathways, Frontiers in cellular neuroscience 9 (2015) 61.
[33] S.J. Reshkin, A. Bellizzi, S. Caldeira, V. Albarani, I. Malanchi, M. Poignee, M. Alunni-Fabbroni, V. Casavola, M. Tommasino, Na+/H+ exchanger-dependent intracellular alkalinization is an early event in malignant transformation and plays an essential role in the

development of subsequent transformation-associated phenotypes, FASEB J 14(14) (2000) 2185-97.
[34] E. Persi, M. Duran-Frigola, M. Damaghi, W.R. Roush, P. Aloy, J.L. Cleveland, R.J. Gillies, E. Ruppin, Systems analysis of intracellular pH vulnerabilities for cancer therapy, Nature communications 9(1) (2018) 2997.
[35] Y. Liu, K.A. White, D.L. Barber, Intracellular pH Regulates Cancer and Stem Cell Behaviors: A Protein Dynamics Perspective, Front Oncol 10 (2020) 1401.
[36] M.J. Gdovin, N. Kadri, L. Rios, S. Holliday, Z. Jordan, Focal photodynamic intracellular acidification as a cancer therapeutic, Semin Cancer Biol 43 (2017) 147-156.
[37] T. Koltai, Triple-edged therapy targeting intracellular alkalosis and extracellular acidosis in cancer, Semin Cancer Biol 43 (2017) 139-146.
[38] C. Zhang, S. Li, A. Yu, Y. Wang, Nano CaCO(3) "Lysosomal Bombs" Enhance Chemotherapy Drug Efficacy via Rebalancing Tumor Intracellular pH, ACS Biomater Sci Eng 5(7) (2019) 3398-3408.
[39] M.J. Yong, B. Kang, U. Yang, S.S. Oh, J.H. Je, Live Streaming of a Single Cell's Life over a Local pH-Monitoring Nanowire Waveguide, Nano Lett 22(15) (2022) 6375-6382.
[40] J.S. Spear, K.A. White, Single-cell intracellular pH dynamics regulate the cell cycle by timing the G1 exit and G2 transition, J Cell Sci 136(10) (2023) jcs260458.
[41] A.M. Porcelli, A. Ghelli, C. Zanna, P. Pinton, R. Rizzuto, M. Rugolo, pH difference across the outer mitochondrial membrane measured with a green fluorescent protein mutant, Biochem Biophys Res Commun 326(4) (2005) 799-804.
[42] J.R. Casey, S. Grinstein, J. Orlowski, Sensors and regulators of intracellular pH, Nat Rev Mol Cell Biol 11(1) (2010) 50-61.
[43] J.J. Rennick, C.J. Nowell, C.W. Pouton, A.P.R. Johnston, Resolving subcellular pH with a quantitative fluorescent lifetime biosensor, Nature communications 13(1) (2022) 6023.
[44] C. Martin, S.F. Pedersen, A. Schwab, C. Stock, Intracellular pH gradients in migrating cells, Am J Physiol Cell Physiol 300(3) (2011) C490-5.
[45] H. Herrmann, I. Hofmann, W.W. Franke, Identification of a nonapeptide motif in the vimentin head domain involved in intermediate filament assembly, J Mol Biol 223(3) (1992) 637-50.
[46] A. Mónico, E. Rodríguez-Senra, F.J. Cañada, S. Zorrilla, D. Pérez-Sala, Drawbacks of dialysis procedures for removal of EDTA, PLoS ONE 12(1) (2017) e0169843.
[47] A. Krezel, W. Maret, The biological inorganic chemistry of zinc ions, Arch Biochem Biophys 611 (2016) 3-19.
[48] S. Kirchhof, A. Strasser, H.J. Wittmann, V. Messmann, N. Hammer, A.M. Goepferich, F.P. Brandl, New insights into the cross-linking and degradation mechanism of Diels-Alder hydrogels, J Mater Chem B 3(3) (2015) 449-457.
[49] A.J. Sarria, J.G. Lieber, S.K. Nordeen, R.M. Evans, The presence or absence of a vimentin-type intermediate filament network affects the shape of the nucleus in human SW-13 cells, J Cell Sci 107 (Pt 6) (1994) 1593-607.
[50] D. Moneo-Corcuera, A. Viedma-Poyatos, K. Stamatakis, D. Pérez-Sala, Desmin Reorganization by Stimuli Inducing Oxidative Stress and Electrophiles: Role of Its Single Cysteine Residue, Antioxidants (Basel) 12(9) (2023) 1703.
[51] M. Koivusalo, C. Welch, H. Hayashi, C.C. Scott, M. Kim, T. Alexander, N. Touret, K.M. Hahn, S. Grinstein, Amiloride inhibits macropinocytosis by lowering submembranous pH and preventing Rac1 and Cdc42 signaling, J Cell Biol 188(4) (2010) 547-63.
[52] K.R. Rogers, H. Herrmann, W.W. Franke, Characterization of disulfide crosslink formation of human vimentin at the dimer, tetramer, and intermediate filament levels, J Struct Biol 117(1) (1996) 55-69.
[53] C.Y. Yang, P.W. Chang, W.H. Hsu, H.C. Chang, C.L. Chen, C.C. Lai, W.T. Chiu, H.C. Chen, Src and SHP2 coordinately regulate the dynamics and organization of vimentin filaments during cell migration, Oncogene 38(21) (2019) 4075-4094.

[54] E.R. Hondorp, R.G. Matthews, Oxidation of cysteine 645 of cobalamin-independent methionine synthase causes a methionine limitation in Escherichia coli, J Bacteriol 191(10) (2009) 3407-10.
[55] P. Vigne, C. Frelin, E.J. Cragoe, Jr., M. Lazdunski, Ethylisopropyl-amiloride: a new and highly potent derivative of amiloride for the inhibition of the Na+/H+ exchange system in various cell types, Biochem Biophys Res Commun 116(1) (1983) 86-90.
[56] D. Pérez-Sala, D. Collado-Escobar, F. Mollinedo, Intracellular Alkalinization Suppresses Lovastatin-induced Apoptosis in HL-60 Cells through the Inactivation of a pH-dependent Endonuclease, J. Biol. Chem. 270(11) (1995) 6235-6242.
[57] C.H. Man, F.E. Mercier, N. Liu, W. Dong, G. Stephanopoulos, L. Jiang, Y. Jung, C.P. Lin, A.Y.H. Leung, D.T. Scadden, Proton export alkalinizes intracellular pH and reprograms carbon metabolism to drive normal and malignant cell growth, Blood 139(4) (2022) 502-522.
[58] A.V. Berezhnov, M.P. Soutar, E.I. Fedotova, M.S. Frolova, H. Plun-Favreau, V.P. Zinchenko, A.Y. Abramov, Intracellular pH Modulates Autophagy and Mitophagy, J Biol Chem 291(16) (2016) 8701-8.
[59] V.K. Capellini, C.B. Restini, L.M. Bendhack, P.R. Evora, A.C. Celotto, The effect of extracellular pH changes on intracellular pH and nitric oxide concentration in endothelial and smooth muscle cells from rat aorta, PLoS One 8(5) (2013) e62887.
[60] D. Kazyken, S.I. Lentz, D.C. Fingar, Alkaline intracellular pH (pHi) activates AMPK-mTORC2 signaling to promote cell survival during growth factor limitation, J Biol Chem 297(4) (2021) 101100.
[61] S. Chung, Y.H. Kim, J.Y. Koh, T.S. Nam, D.S. Ahn, Intracellular acidification evoked by moderate extracellular acidosis attenuates transient receptor potential V1 (TRPV1) channel activity in rat dorsal root ganglion neurons, Exp Physiol 96(12) (2011) 1270-81.
[62] F.J. Sánchez-Gómez, B. Díez-Dacal, M.A. Pajares, O. Llorca, D. Pérez-Sala, Cyclopentenone prostaglandins with dienone structure promote cross-linking of the chemoresistance-inducing enzyme Glutathione Transferase P1-1, Mol Pharmacol 78 (2010) 723-733.
[63] K. Rokutan, R.B. Johnston, Jr., K. Kawai, Oxidative stress induces S-thiolation of specific proteins in cultured gastric mucosal cells, Am J Physiol 266(2 Pt 1) (1994) G247-54.
[64] M.A. Yusuf, T. Chuang, G.J. Bhat, K.S. Srivenugopal, Cys-141 glutathionylation of human p53: Studies using specific polyclonal antibodies in cancer samples and cell lines, Free Radic Biol Med 49(5) (2010) 908-17.
[65] M. Fratelli, H. Demol, M. Puype, S. Casagrande, I. Eberini, M. Salmona, V. Bonetto, M. Mengozzi, F. Duffieux, E. Miclet, A. Bachi, J. Vandekerckhove, E. Gianazza, P. Ghezzi, Identification by redox proteomics of glutathionylated proteins in oxidatively stressed human T lymphocytes, Proc Natl Acad Sci U S A 99 (2002) 3505-3510.
[66] B.Y.K. Yu, M.A. Tossounian, S.D. Hristov, R. Lawrence, P. Arora, Y. Tsuchiya, S.Y. Peak-Chew, V. Filonenko, S. Oxenford, R. Angell, J. Gouge, M. Skehel, I. Gout, Regulation of metastasis suppressor NME1 by a key metabolic cofactor coenzyme A, Redox Biol 44 (2021) 101978.
[67] S. Duarte, T. Melo, R. Domingues, J.d.D. Alché, D. Pérez-Sala, Insight into the cellular effects of nitrated phospholipids: evidence for pleiotropic mechanisms of action, Free Rad Biol Med 144 (2019) 192-202.
[68] I. Lois-Bermejo, P. González-Jiménez, S. Duarte, M.A. Pajares, D. Pérez-Sala, Vimentin tail segments are differentially exposed at distinct cellular locations and in response to stress, Frontiers in cell and developmental biology 10 (2022) 908263.
[69] C.H. Kaschula, R. Tuveri, E. Ngarande, K. Dzobo, C. Barnett, D.A. Kusza, L.M. Graham, A.A. Katz, M.S. Rafudeen, M.I. Parker, R. Hunter, G. Schafer, The garlic compound ajoene covalently binds vimentin, disrupts the vimentin network and exerts anti-metastatic activity in cancer cells, BMC Cancer 19(1) (2019) 248.

[70] G. Ferrer-Sueta, B. Manta, H. Botti, R. Radi, M. Trujillo, A. Denicola, Factors affecting protein thiol reactivity and specificity in peroxide reduction, Chem Res Toxicol 24(4) (2011) 434-50.
[71] G. Gambardella, G. Cattani, A. Bocedi, G. Ricci, New Factors Enhancing the Reactivity of Cysteines in Molten Globule-Like Structures, International journal of molecular sciences 21(18) (2020) 6949.
[72] G. Roos, N. Foloppe, J. Messens, Understanding the pK(a) of redox cysteines: the key role of hydrogen bonding, Antioxid Redox Signal 18(1) (2013) 94-127.
[73] L.B. Poole, The basics of thiols and cysteines in Redox Biol and chemistry, Free Radic Biol Med 80 (2015) 148-57.
[74] A. Groen, S. Lemeer, T. van der Wijk, J. Overvoorde, A.J. Heck, A. Ostman, D. Barford, M. Slijper, J. den Hertog, Differential oxidation of protein-tyrosine phosphatases, J Biol Chem 280 (2005) 10298-10304.
[75] S.C. Jao, S.M. English Ospina, A.J. Berdis, D.W. Starke, C.B. Post, J.J. Mieyal, Computational and mutational analysis of human glutaredoxin (thioltransferase): probing the molecular basis of the low pKa of cysteine 22 and its role in catalysis, Biochemistry 45(15) (2006) 4785-96.
[76] D. Pérez-Sala, R. Quinlan, The redox-responsive roles of intermediate filaments in cellular stress detection, integration and mitigation, Curr Opin Cell Biol 86 (2024) 102283.
[77] M. Flinck, S.H. Kramer, S.F. Pedersen, Roles of pH in control of cell proliferation, Acta Physiol (Oxf) 223(3) (2018) e13068.
[78] L.M. Koharudin, H. Liu, R. Di Maio, R.B. Kodali, S.H. Graham, A.M. Gronenborn, Cyclopentenone prostaglandin-induced unfolding and aggregation of the Parkinson disease-associated UCH-L1, Proc Natl Acad Sci U S A 107(15) (2010) 6835-40.
[79] C.A. Lemmon, T. Ohashi, H.P. Erickson, Probing the folded state of fibronectin type III domains in stretched fibrils by measuring buried cysteine accessibility, J Biol Chem 286(30) (2011) 26375-82.
[80] J. Alegre-Cebollada, P. Kosuri, D. Giganti, E. Eckels, J.A. Rivas-Pardo, N. Hamdani, C.M. Warren, R.J. Solaro, W.A. Linke, J.M. Fernandez, S-glutathionylation of cryptic cysteines enhances titin elasticity by blocking protein folding, Cell 156(6) (2014) 1235-1246.
[81] C.P. Johnson, H.Y. Tang, C. Carag, D.W. Speicher, D.E. Discher, Forced unfolding of proteins within cells, Science 317(5838) (2007) 663-6.
[82] J. Swift, I.L. Ivanovska, A. Buxboim, T. Harada, P.C. Dingal, J. Pinter, J.D. Pajerowski, K.R. Spinler, J.W. Shin, M. Tewari, F. Rehfeldt, D.W. Speicher, D.E. Discher, Nuclear lamin-A scales with tissue stiffness and enhances matrix-directed differentiation, Science 341(6149) (2013) 1240104.
[83] B. Pedre, D. Talwar, U. Barayeu, D. Schilling, M. Luzarowski, M. Sokolowski, S. Glatt, T.P. Dick, 3-Mercaptopyruvate sulfur transferase is a protein persulfidase, Nat Chem Biol 19(4) (2023) 507-517.
[84] S. López-Ongil, G. Torrecillas, D. Pérez-Sala, L. González-Santiago, M. Rodríguez-Puyol, D. Rodríguez-Puyol, Mechanisms involved in the contraction of endothelial cells by hydrogen peroxide, Free Rad. Biol. Med. 26 (1999) 501-510.
[85] J. Huot, F. Houle, F. Marceau, J. Landry, Oxidative stress-induced actin reorganization mediated by the p38 mitogen-activated protein kinase/heat shock protein 27 pathway in vascular endothelial cells, Circ Res 80(3) (1997) 383-92.
[86] M. Damaghi, J.W. Wojtkowiak, R.J. Gillies, pH sensing and regulation in cancer, Frontiers in physiology 4 (2013) 370.
[87] N. Yonezawa, E. Nishida, H. Sakai, pH control of actin polymerization by cofilin, J Biol Chem 260(27) (1985) 14410-2.
[88] C. Frantz, G. Barreiro, L. Dominguez, X. Chen, R. Eddy, J. Condeelis, M.J. Kelly, M.P. Jacobson, D.L. Barber, Cofilin is a pH sensor for actin free barbed end formation: role of phosphoinositide binding, J Cell Biol 183(5) (2008) 865-79.

[89] F. Cuello, P. Eaton, Cysteine-Based Redox Sensing and Its Role in Signaling by Cyclic Nucleotide-Dependent Kinases in the Cardiovascular System, Annu Rev Physiol 81 (2019) 63-87.
[90] D.P. Byrne, S. Shrestha, M. Galler, M. Cao, L.A. Daly, A.E. Campbell, C.E. Eyers, E.A. Veal, N. Kannan, P.A. Eyers, Aurora A regulation by reversible cysteine oxidation reveals evolutionarily conserved redox control of Ser/Thr protein kinase activity, Science signaling 13(639) (2020) eaax2713.
[91] J.E. Eriksson, T. He, A.V. Trejo-Skalli, A.-S. Härmälä-Braskén, J. Hellman, Y.-H. Chou, R.D. Goldman, Specific in vivo phosphorylation sites determine the assembly dynamics of vimentin intermediate filaments, J Cell Sci 117 (2004) 919-932.
[92] M. Lakemeyer, M. Bogyo, Uncovering an overlooked consequence of phosphorylation: change in cysteine reactivity, Nat Methods 19(3) (2022) 281-283.
[93] E.K. Kemper, Y. Zhang, M.M. Dix, B.F. Cravatt, Global profiling of phosphorylation-dependent changes in cysteine reactivity, Nat Methods 19(3) (2022) 341-352.
[94] M.C. Xia, L. Cai, S. Zhang, X. Zhang, A cell-penetrating ratiometric probe for simultaneous measurement of lysosomal and cytosolic pH change, Talanta 178 (2018) 355-361.
[95] Q. Hu, Y. Xia, S. Corda, J.L. Zweier, R.C. Ziegelstein, Hydrogen peroxide decreases pHi in human aortic endothelial cells by inhibiting Na+/H+ exchange, Circ Res 83(6) (1998) 644-51.
[96] R.S. Funk, J.P. Krise, Exposure of cells to hydrogen peroxide can increase the intracellular accumulation of drugs, Mol Pharm 4(1) (2007) 154-9.
[97] B. Díez-Dacal, D. Pérez-Sala, Anti-inflammatory prostanoids: focus on the interactions between electrophile signalling and resolution of inflammation, The Scientific World Journal 10 (2010) 655-675.
[98] A. Viedma-Poyatos, P. Gonzalez-Jimenez, O. Langlois, I. Company-Marin, C.M. Spickett, D. Perez-Sala, Protein Lipoxidation: Basic Concepts and Emerging Roles, Antioxidants (Basel) 10(2) (2021) e1009128.
[99] A.V. Schepers, C. Lorenz, S. Koster, Tuning intermediate filament mechanics by variation of pH and ion charges, Nanoscale 12(28) (2020) 15236-15245.
[100] S.W. Griffiths, J. King, C.L. Cooney, The reactivity and oxidation pathway of cysteine 232 in recombinant human alpha 1-antitrypsin, J Biol Chem 277(28) (2002) 25486-92.
[101] V.V. Pak, D. Ezerina, O.G. Lyublinskaya, B. Pedre, P.A. Tyurin-Kuzmin, N.M. Mishina, M. Thauvin, D. Young, K. Wahni, S.A. Martinez Gache, A.D. Demidovich, Y.G. Ermakova, Y.D. Maslova, A.G. Shokhina, E. Eroglu, D.S. Bilan, I. Bogeski, T. Michel, S. Vriz, J. Messens, V.V. Belousov, Ultrasensitive Genetically Encoded Indicator for Hydrogen Peroxide Identifies Roles for the Oxidant in Cell Migration and Mitochondrial Function, Cell Metab 31(3) (2020) 642-653 e6.
[102] M.E. Kidd, D.K. Shumaker, K.M. Ridge, The role of vimentin intermediate filaments in the progression of lung cancer, Am J Respir Cell Mol Biol 50(1) (2014) 1-6.

Figure legends

Figure 1. Modification of vimentin cysteine in vitro is sensitive to pH. Purified recombinant vimentin at 4 µM was incubated with various oxidants or cysteine reactive compounds, as follows: (A) H_2O_2 1 mM for 1 h; (B) 1 mM diamide for 1 h or (C) Mal-B for 15 min. Aliquots from the incubation mixtures were analyzed by gel electrophoresis under non-reducing or reducing conditions, as indicated. In A and B protein species were detected by total protein staining with Sypro Ruby. The position of the vimentin oligomers is indicated by an arrowhead. In (C), biotin incorporation was assessed by electrotransfer to Immobilon-P membranes and detection with HRP-streptavidin, whereas vimentin was detected with antibodies. Graphs at the bottom show quantitations of vimentin oligomer levels or of biotinylated vimentin. (D) Purified vimentin was incubated in the absence or presence of diamide at different pH, as indicated in the assay outline, and subjected to polymerization with NaCl. Subsequently, vimentin structures were visualized by immunodetection and fluorescence microscopy. Samples treated with diamide at pH 8.0, but without vimentin or without antibodies (bright field image), as indicated, are shown at the far right. 2nd antibody-488, secondary antibody conjugated with Alexa488.

Figure 2. The disruption of the vimentin network elicited by diamide is modulated by pH in cells. (A) SW13/cl.2 cells stably expressing vimentin wt were treated with 1 mM diamide for the indicated time periods and vimentin reorganization was assessed by immunofluorescence (scale bar 20 µm). The fluorescence intensity profiles along the dotted lines drawn on images from 15 min and 2 h treatments are depicted in the graph at the right in order to illustrate the increase in cytoplasmic background related to vimentin disassembly. (B) Cells were incubated in culture media at different pH, supplemented with nigericin as indicated, and treated in the absence or presence of 1 mM diamide for 15 min. Vimentin was visualized by immunofluorescence (scale bars, 20 µm). (C) SW13/cl.2 cells transfected with mCherry-SEpHluorin were incubated in media at different pH as in (B), and after 15 min, intracellular pH was estimated from the ratio of the green/red fluorescence, as detailed in the experimental section (scale bars, 20 µm). (D) Lysates from SW13/cl.2 expressing vimentin wt treated as in (A) were analyzed by western blot with anti-vimentin antibodies directed to the amino terminal (D21H3, left images) or to the carboxyl terminal (V9, right images) to assess the levels and electrophoretical mobility of the protein.

Figure 3. Effect of variations in pH on the disruption of other cytoskeletal structures by diamide. SW13/cl.2 cells stably expressing vimentin wt were incubated in culture media at various pH supplemented with nigericin as indicated and treated in the absence or presence of 1 mM diamide for 15 min. At the end of the treatment cells were fixed and stained with TRITC-phalloidin to visualize f-actin (A and B) or subjected to immunofluorescence with anti-tubulin and anti-vimentin antibodies. (A) The typical reorganization of f-actin elicited by diamide is illustrated. Insets show the position of nuclei stained with DAPI. Fluorescence intensity profiles along the dotted lines drawn on images are shown in the graph below to illustrate the decrease in f-actin staining coinciding with the nuclear region. (B) Representative images of actin alterations under the various experimental conditions are shown. Enlarged views of areas of interest delimited by dotted squares are depicted at the right of each image. (C) Representative images of tubulin alterations are shown (cyan) and the vimentin staining in the same cells is shown at the right of each image (green). Scale bars, 20 µm

Figure 4. Pharmacological modulation of pHi influences diamide-elicited vimentin disruption. SW13/cl.2 cells stably expressing vimentin wt were treated in the absence or presence of 1 mM diamide for 15 min after preincubation with 25 µM EIPA for 15 min, 10 µM syrosingopine for 1 h, or 10 µM monensin for 5 min. (A) The reorganization of vimentin was assessed by

immunofluorescence (scale bars, 20 µm). (B) The extent of the reorganization was assessed by counting the number of filament fragments per cell. One-way analysis of variance (ANOVA) followed by Tukey's multiple comparison test was used for statistical analysis. Three independent experiments were carried out and six cells from each one were evaluated. Data shown are mean values ± SEM. Statistically significant differences are indicated on the graphs, as follows: **p<0.01; ****p<0.0001. (C) SW13/cl.2 cells transfected with mCherry-SEpHluorin were treated as in (A). At the end of the treatments, variations in pHi were estimated from the ratio of green to red fluorescence, as described in the experimental section. For statistical analysis, 10 cells per experiment (n=3) were evaluated. Data shown are mean values ± SEM. Statistically significant differences correspond to *p<0.05; ***p<0.001; ****p<0.0001 by one-way analysis of variance (ANOVA) followed by Tukey's multiple comparison test

Figure 5. The extent of modification of vimentin C328 in cells depend on pHi. (A) Scheme of the strategy employed to estimate the extent of modification of C328. Cells are treated with the compounds of interest, e.g., diamide, and then lysed in the presence or absence of biotinylated maleimide (Maleimide-biotin, Mal-B) to label free thiols. Total cell lysates are subjected to vimentin immunoprecipitation with V9-agarose, and immunoprecipitates analyzed for biotin and vimentin detection as detailed in the experimental section. A higher incorporation of Mal-B is expected when cellular vimentin C328 is mainly in its free thiol form, whereas a lower Mal-B signal would indicate a higher degree of oxidation or modification in cells under the conditions of the treatment. (B) SW13/cl.2 cells stably expressing vimentin wt were treated in the absence or presence of 1 mM diamide for 15 min and processed according to the scheme in (A). The biotinylated polypeptide comigrating with vimentin is marked by an arrowhead. The dashed line indicates where lanes from the same gel have been cropped. The graph in the lower panel depicts the quantitation of biotin incorporation into the vimentin band, corrected by vimentin levels and expressed with respect to the control condition. Results are average values ± S.E.M. of four independent experiments. ***p<0.001 versus control. (C) Cells were pretreated with vehicle, 25 µM EIPA for 15 min or 10 µM monensin for 5 min before incubation with diamide, as above. Cells were processed as described in (A) and levels of biotin incorporation quantitated as described in (B). Results are average values ± S.E.M. of two independent experiments.

Figure 6. The disruption of the vimentin network elicited by diamide is modulated by pH in several cell types. Hela cells (A) or human primary fibroblasts (B) were incubated in culture media at various pH supplemented with nigericin as indicated, or pretreated with 25 µM EIPA for 15 min, or 10 µM monensin for 5 min, before treatment in the absence or presence of 1 mM diamide for 15 min. The distribution of vimentin was assessed by immunofluorescence (scale bars, 20 µm). In (B), images on the left for each condition are overall projections. Enlarged views of areas of interest delimited by dotted squares are depicted at the right of each image, as single sections.

Figure 7. Importance of the vimentin single cysteine residue, C328, in the disruption by diamide at different pH. SW13/cl.2 cells expressing the vimentin C328A mutant were incubated in culture media at different pH supplemented with nigericin as indicated, or pretreated with 10 µM monensin for 5 min, before treatment in the absence or presence of 1 mM diamide for 15 min. The distribution of vimentin filaments was assessed by immunofluorescence (A) and that of f-actin by staining with TRITC-phalloidin (B).

Figure 8. Scheme of the putative changes in cysteine ionization and modification depending on the cysteine pKa and the pH of the environment.

Figure 1

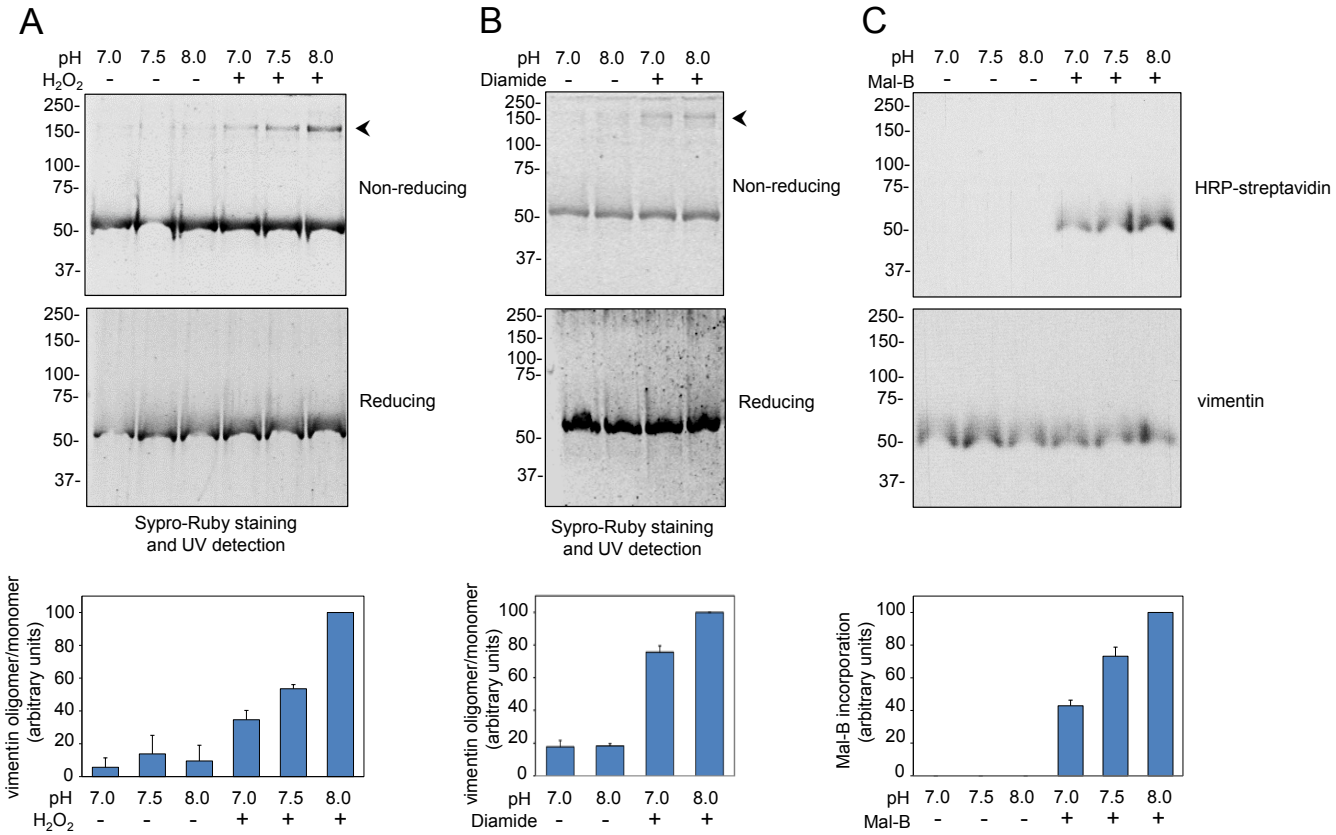
A
pH 7.0 7.5 8.0 7.0 7.5 8.0
H2O2 - - - + + +
250-
150-
100-
75-
50-
37-
Non-reducing
Reducing
Sypro-Ruby staining and UV detection
vimentin oligomer/monomer (arbitrary units)
B
pH 7.0 8.0 7.0 8.0
Diamide - - + +
Non-reducing
Reducing
Sypro-Ruby staining and UV detection
vimentin oligomer/monomer (arbitrary units)
C
pH 7.0 7.5 8.0 7.0 7.5 8.0
Mal-B - - - + + +
HRP-streptavidin
vimentin
Mal-B incorporation (arbitrary units)

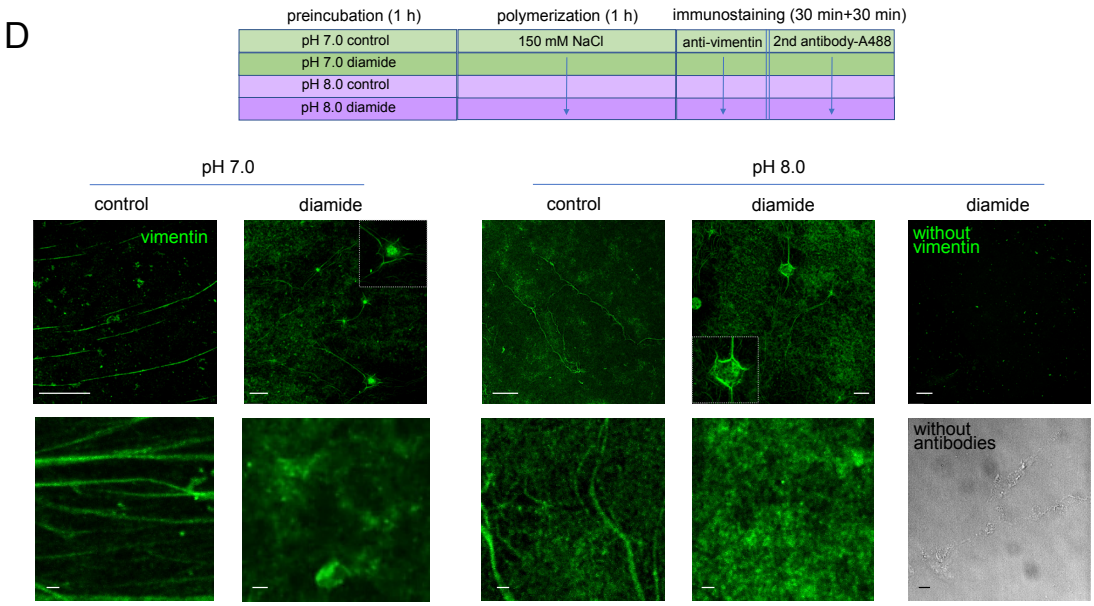
D
preincubation (1 h)
polymerization (1 h)
immunostaining (30 min+30 min)
pH 7.0 control
pH 7.0 diamide
pH 8.0 control
pH 8.0 diamide
150 mM NaCl
anti-vimentin
2nd antibody-A488
pH 7.0
pH 8.0
control
diamide
control
diamide
diamide
vimentin
without vimentin
without antibodies

Figure 2

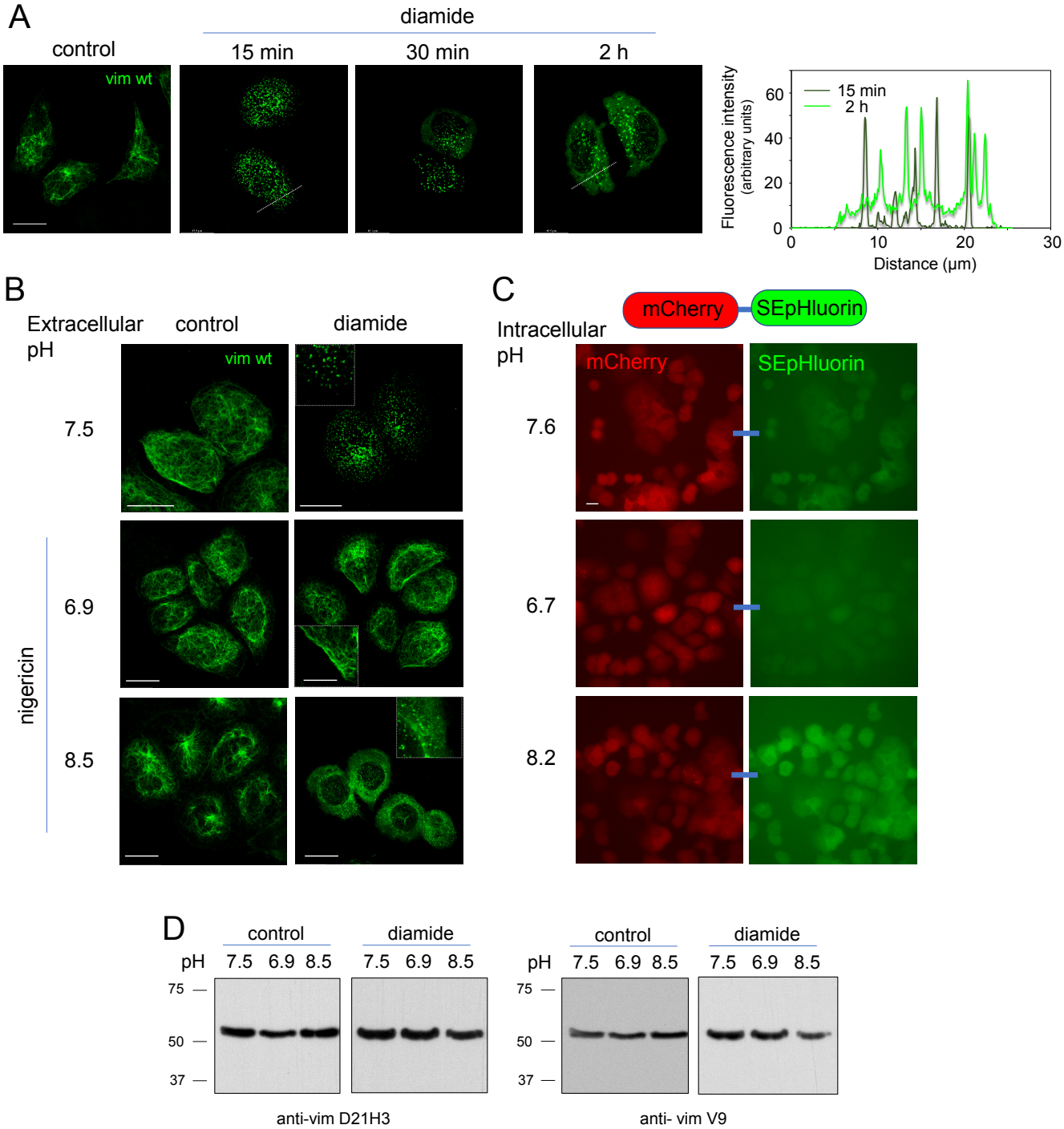
A
diamide
control
15 min
30 min
2 h
vim wt
Fluorescence intensity (arbitrary units)
15 min
2 h
Distance (µm)
B
Extracellular pH
control
diamide
vim wt
7.5
6.9
8.5
nigericin
C
mCherry
SEpHluorin
Intracellular pH
7.6
6.7
8.2
D
control
diamide
pH
7.5 6.9 8.5
75
50
37
anti-vim D21H3
anti- vim V9

Figure 3

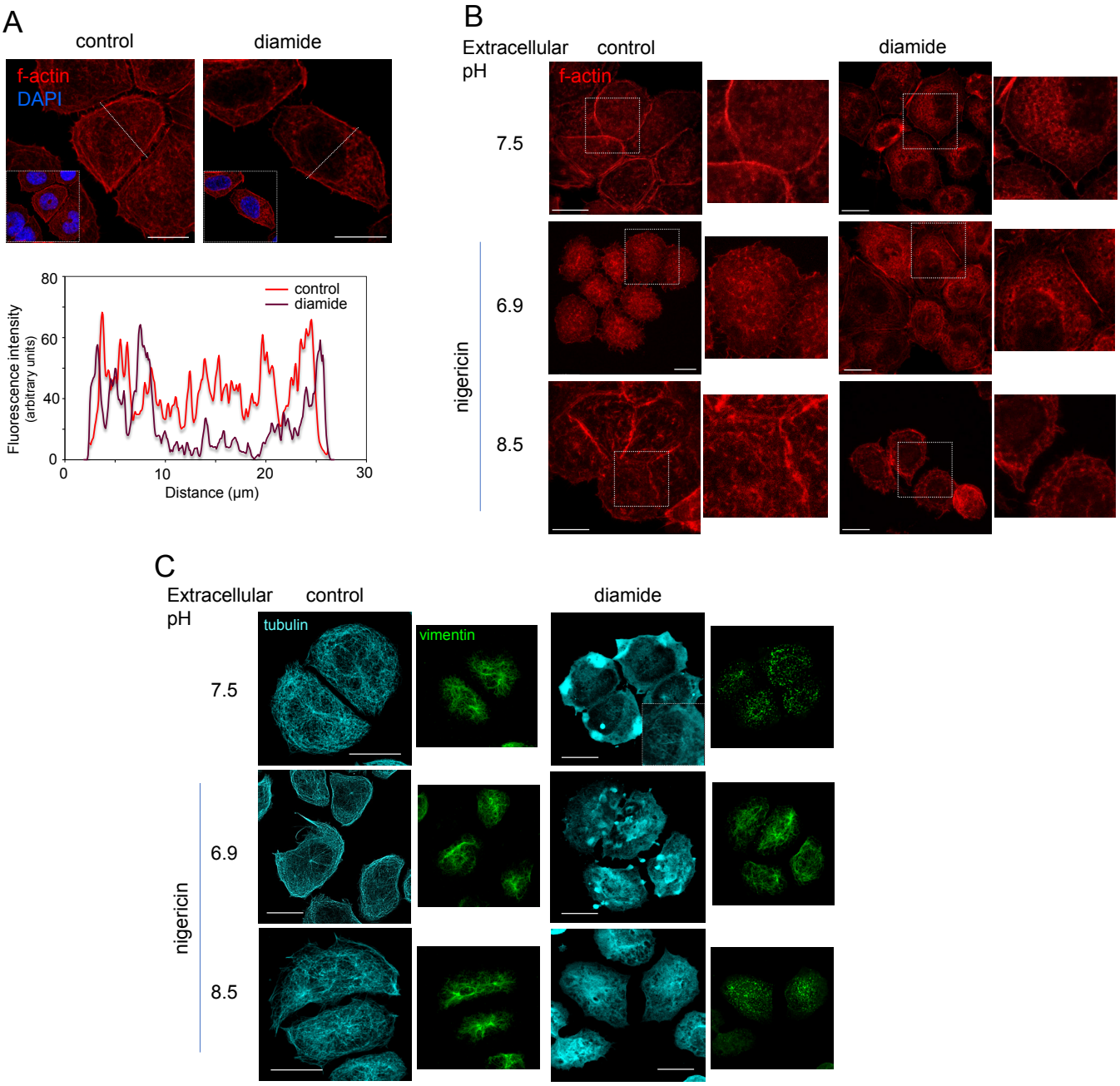
A
control
diamide
f-actin
DAPI
Fluorescence intensity (arbitrary units)
Distance (μm)
control
diamide
B
Extracellular pH
control
diamide
f-actin
7.5
6.9
8.5
nigericin
C
Extracellular pH
control
diamide
tubulin
vimentin
7.5
6.9
8.5
nigericin

Figure 4

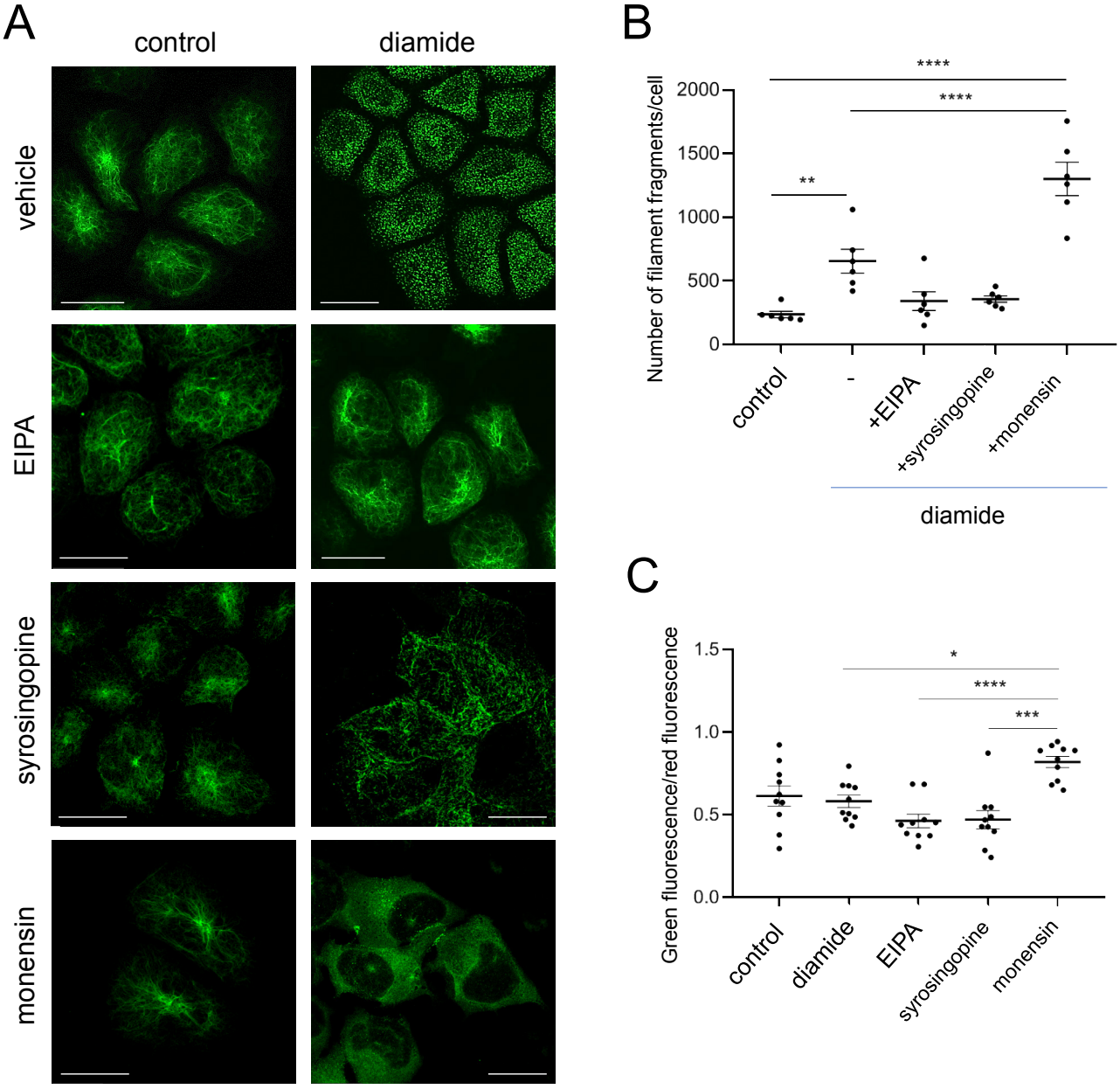
A
control
diamide
vehicle
EIPA
syrosingopine
monensin
B
Number of filament fragments/cell
2000
1500
1000
500
0
****
****
**
control
-
+EIPA
+syrosingopine
+monensin
diamide
C
Green fluorescence/red fluorescence
1.5
1.0
0.5
0.0
*
****
***
control
diamide
EIPA
syrosingopine
monensin

Figure 5

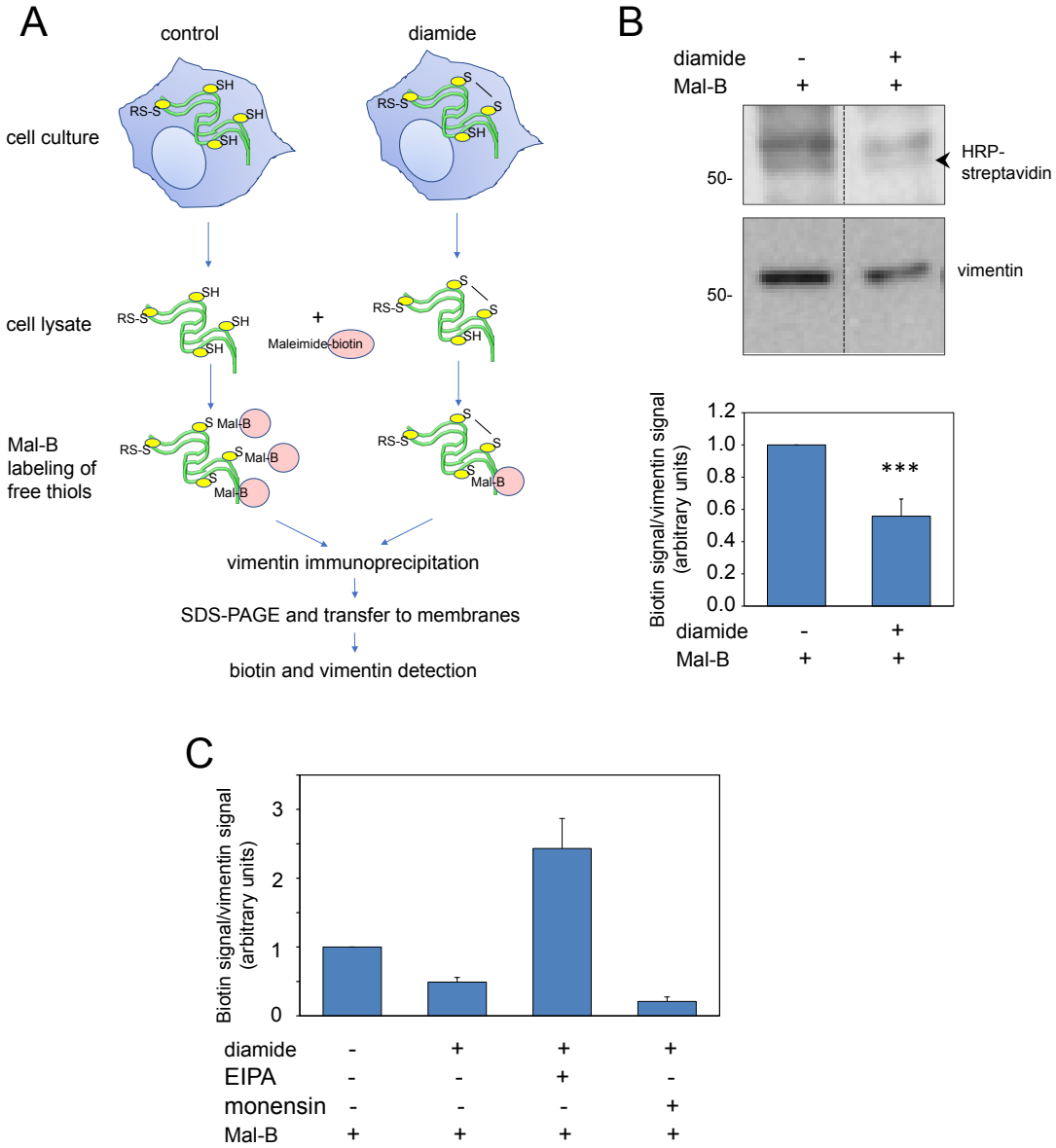
A
control
diamide
cell culture
cell lysate
Mal-B
labeling of
free thiols
RS-S
SH
S
Mal-B
+
Maleimide-biotin
vimentin immunoprecipitation
SDS-PAGE and transfer to membranes
biotin and vimentin detection
B
diamide - +
Mal-B + +
50-
HRP-
streptavidin
vimentin
Biotin signal/vimentin signal
(arbitrary units)
1.2
1.0
0.8
0.6
0.4
0.2
0.0
***
diamide - +
Mal-B + +
C
Biotin signal/vimentin signal
(arbitrary units)
3
2
1
0
diamide - + + +
EIPA - - + -
monensin - - - +
Mal-B + + + +

Figure 6

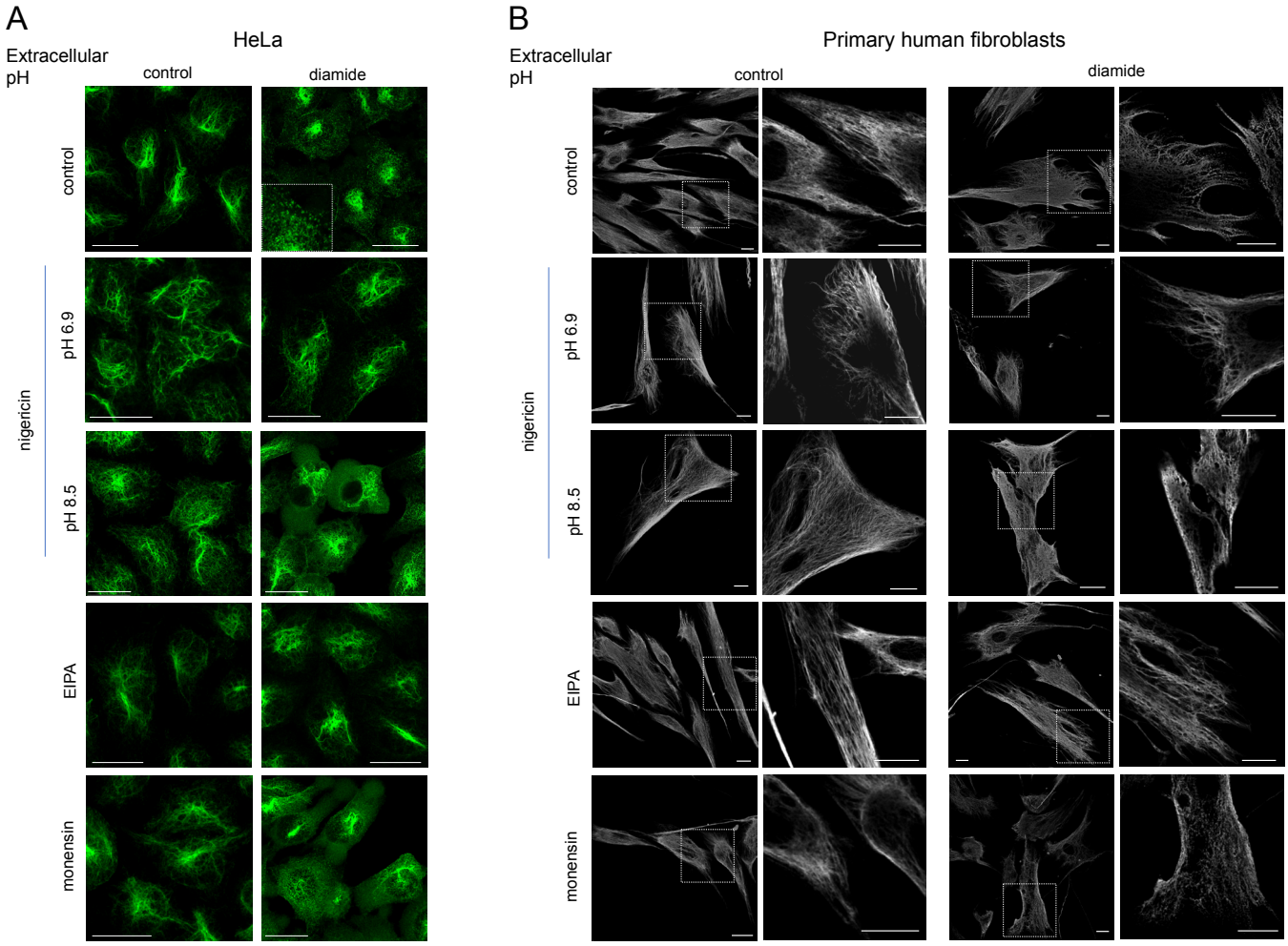
A
HeLa
Extracellular pH
control
diamide
control
nigericin
pH 6.9
pH 8.5
EIPA
monensin
B
Primary human fibroblasts
Extracellular pH
control
diamide
control
nigericin
pH 6.9
pH 8.5
EIPA
monensin

Figure 7

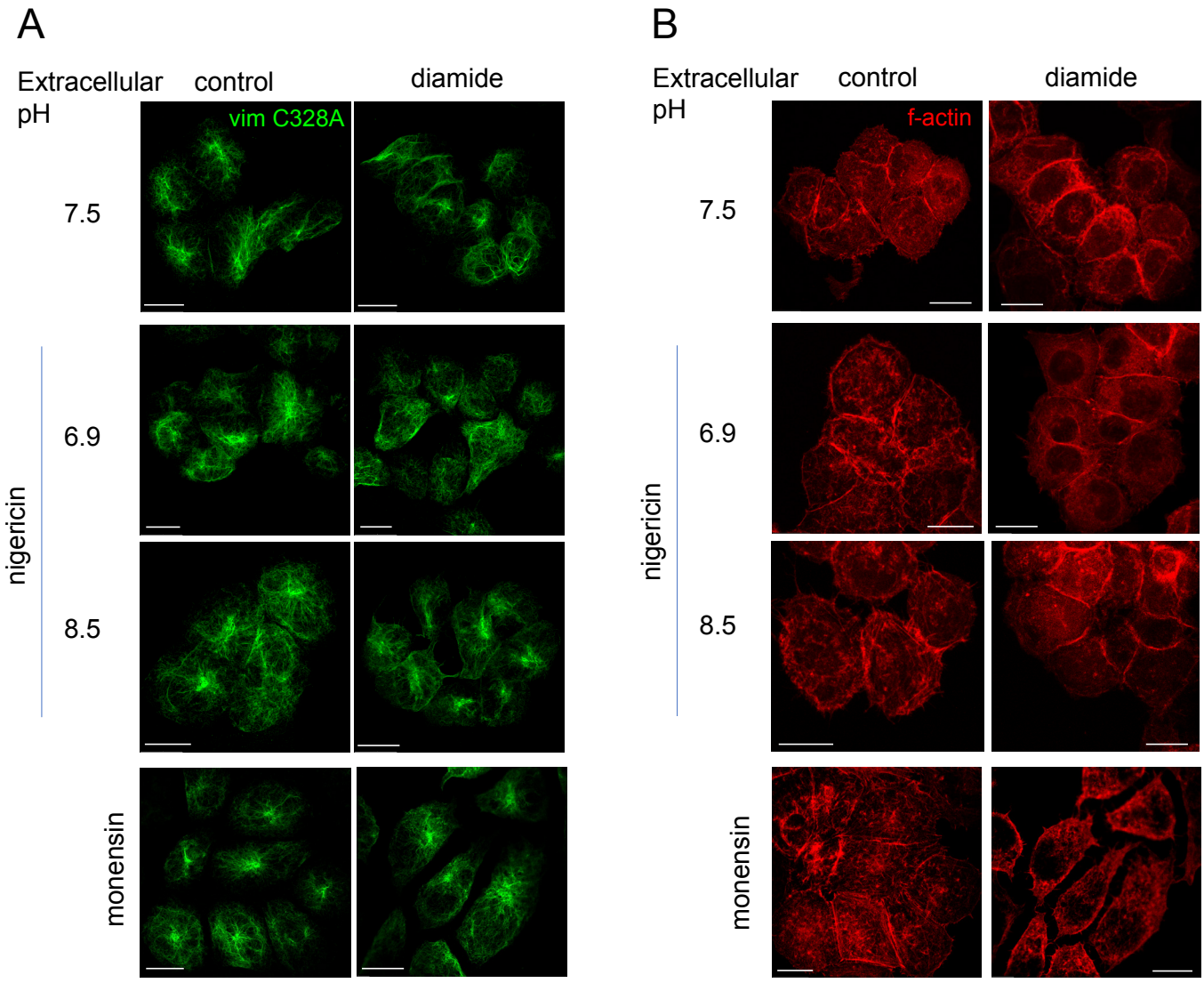
A
Extracellular pH
control
diamide
vim C328A
7.5
6.9
8.5
nigericin
monensin
B
Extracellular pH
control
diamide
f-actin
7.5
6.9
8.5
nigericin
monensin

Figure 8

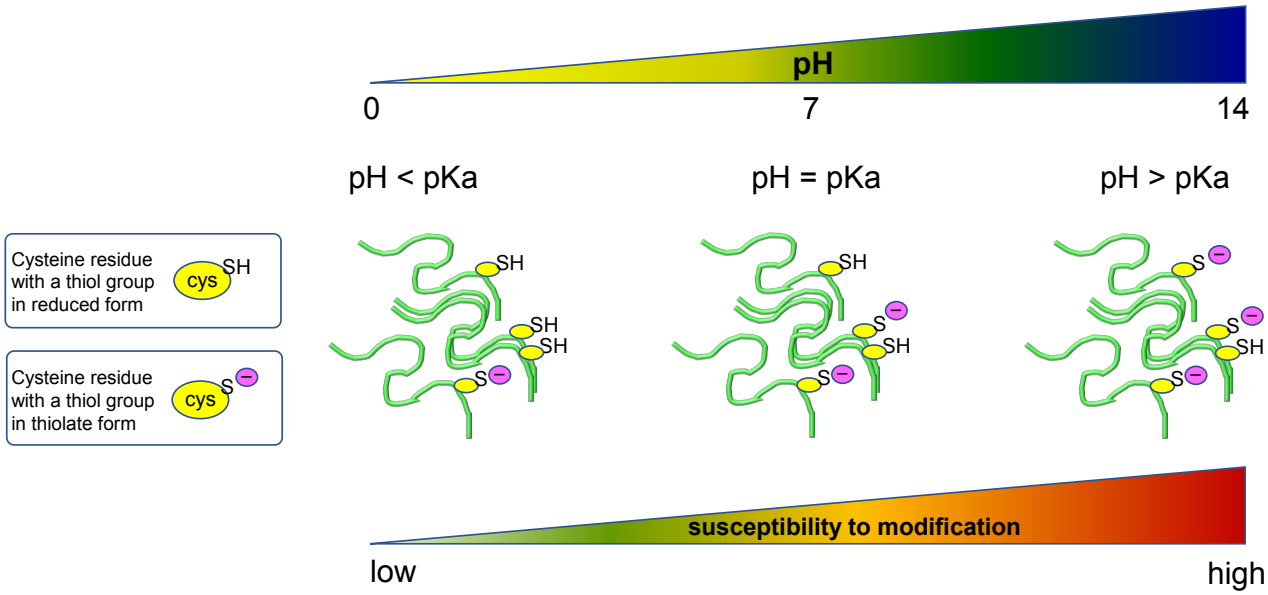
pH
0
7
14
pH < pKa
pH = pKa
pH > pKa
Cysteine residue with a thiol group in reduced form
cys
SH
Cysteine residue with a thiol group in thiolate form
cys
S
SH
S
susceptibility to modification
low
high